
Flamingo: a Visual Language Model for Few-Shot Learning

Jean-Baptiste Alayrac^{*,†} Jeff Donahue^{*} Pauline Luc^{*} Antoine Miech^{*}
 Iain Barr[†] Yana Hasson[†] Karel Lenc[†] Arthur Mensch[†] Katie Millican[†]
 Malcolm Reynolds[†] Roman Ring[†] Eliza Rutherford[†] Serkan Cabi Tengda Han
 Zhitao Gong Sina Samangooei Marianne Monteiro Jacob Menick
 Sebastian Borgeaud Andrew Brock Aida Nematzadeh Sahand Sharifzadeh
 Mikolaj Binkowski Ricardo Barreira Oriol Vinyals Andrew Zisserman
 Karen Simonyan^{*,‡}

* Equal contributions, ordered alphabetically, † Equal contributions, ordered alphabetically,
 ‡ Equal senior contributions

DeepMind

Abstract

Building models that can be rapidly adapted to novel tasks using only a handful of annotated examples is an open challenge for multimodal machine learning research. We introduce Flamingo, a family of Visual Language Models (VLM) with this ability. We propose key architectural innovations to: (i) bridge powerful pretrained vision-only and language-only models, (ii) handle sequences of arbitrarily interleaved visual and textual data, and (iii) seamlessly ingest images or videos as inputs. Thanks to their flexibility, Flamingo models can be trained on large-scale multimodal web corpora containing arbitrarily interleaved text and images, which is key to endow them with in-context few-shot learning capabilities. We perform a thorough evaluation of our models, exploring and measuring their ability to rapidly adapt to a variety of image and video tasks. These include open-ended tasks such as visual question-answering, where the model is prompted with a question which it has to answer; captioning tasks, which evaluate the ability to describe a scene or an event; and close-ended tasks such as multiple-choice visual question-answering. For tasks lying anywhere on this spectrum, a *single* Flamingo model can achieve a new state of the art with few-shot learning, simply by prompting the model with task-specific examples. On numerous benchmarks, *Flamingo* outperforms models fine-tuned on thousands of times more task-specific data.

Corresponding authors: {jalayrac|jeffdonahue|paulineluc|miech}@deepmind.com
 36th Conference on Neural Information Processing Systems (NeurIPS 2022).

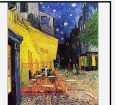
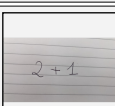
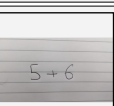
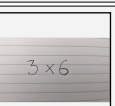
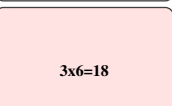
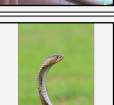
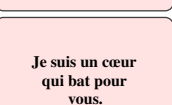
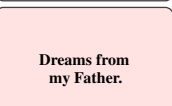
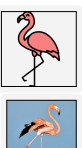
Input Prompt	Completion		
 <p>This is a chinchilla. They are mainly found in Chile.</p>  <p>This is a shiba. They are very popular in Japan.</p>  <p>This is</p>	 <p>a flamingo. They are found in the Caribbean and South America.</p>		
 <p>What is the title of this painting? Answer: The Hallucinogenic Toreador.</p>  <p>Where is this painting displayed? Answer: Louvre Museum, Paris.</p>  <p>What is the name of the city where this was painted? Answer:</p>	 <p>Arles.</p>		
 <p>Output: "Underground"</p>  <p>Output: "Congress"</p>  <p>Output:</p>	 <p>"Soulomes"</p>		
 <p>2+1=3</p>  <p>5+6=11</p>  <p>3x6</p>	 <p>3x6=18</p>		
 <p>Output: A propaganda poster depicting a cat dressed as French emperor Napoleon holding a piece of cheese.</p>  <p>Output: A pink room with a flamingo pool float.</p>  <p>Output:</p>	 <p>A portrait of Salvador Dali with a robot head.</p>		
 <p>Les sanglots longs des violons de l'automne blessent mon cœur d'une langueur monotone.</p>  <p>Pour qui sont ces serpents qui sifflent sur vos têtes?</p>  <p>Output:</p>	 <p>Je suis un cœur qui bat pour vous.</p>		
 <p>pandas: 3</p>  <p>dogs: 2</p>  <p>giraffes: 4</p>			
<p>I like reading</p>  <p>, my favourite play is Hamlet. I also like</p>  <p>, my favorite book is</p>	 <p>Dreams from my Father.</p>		
 <p>What happens to the man after hitting the ball? Answer:</p>	 <p>he falls down.</p>		
 <p>This is a picture of two teddy bears on the moon.</p> <p>What are they doing? They are having a conversation.</p> <p>What object are they using? It looks like a computer.</p> <p>Is this surprising? Yes, it is surprising.</p> <p>Why is this picture surprising to you? I think it is surprising because teddy bears are not usually found on the moon.</p>	 <p>What is the common thing about these three images? They are all flamingos.</p> <p>What is the difference between these three images? The first one is a cartoon, the second one is a real flamingo, and the third one is a 3D model of a flamingo.</p>	 <p>This is an apple with a sticker on it. What does the sticker say? The sticker says "iPod".</p> <p>Where is the photo taken? It looks like it's taken in a backyard.</p> <p>Do you think it is printed or handwritten? It looks like it's handwritten.</p> <p>What color is the sticker? It's white.</p>	 <p>This is a cityscape. It looks like Chicago.</p> <p>What makes you think this is Chicago? I think it's Chicago because of the Shedd Aquarium in the background.</p>  <p>What about this one? Which city is this and what famous landmark helped you recognise the city? This is Tokyo. I think it's Tokyo because of the Tokyo Tower.</p>

Figure 1: Selected examples of inputs and outputs obtained from *Flamingo-80B*. *Flamingo* can rapidly adapt to various image/video understanding tasks with few-shot prompting (top). Out of the box, *Flamingo* is also capable of multi-image visual dialogue (bottom). More examples in Appendix C.

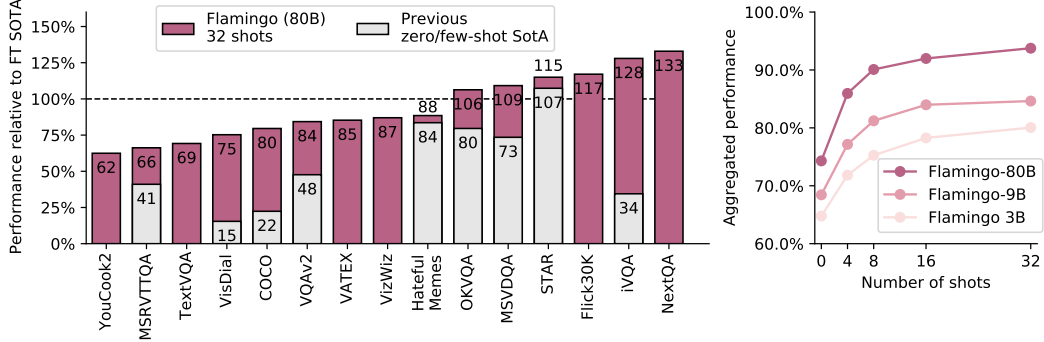


Figure 2: **Flamingo results overview.** *Left:* Our largest model, dubbed *Flamingo*, outperforms state-of-the-art fine-tuned models on 6 of the 16 tasks we consider with no fine-tuning. For the 9 tasks with published few-shot results, *Flamingo* sets the new few-shot state of the art. *Note:* We omit RareAct, our 16th benchmark, as it is a zero-shot benchmark with no available fine-tuned results to compare to. *Right:* Flamingo performance improves with model size and number of shots.

1 Introduction

One key aspect of intelligence is the ability to quickly learn to perform a new task given a short instruction [33, 70]. While initial progress has been made towards a similar capability in computer vision, the most widely used paradigm still consists of first pretraining on a large amount of supervised data, before fine-tuning the model on the task of interest [66, 118, 143]. However, successful fine-tuning often requires many thousands of annotated data points. In addition, it often requires careful per-task hyperparameter tuning and is also resource intensive. Recently, multimodal vision-language models trained with a contrastive objective [50, 85] have enabled zero-shot adaptation to novel tasks, without the need for fine-tuning. However, because these models simply provide a similarity score between a text and an image, they can only address limited use cases such as classification, where a finite set of outcomes is provided beforehand. They crucially lack the ability to generate language, which makes them less suitable to more open-ended tasks such as captioning or visual question-answering. Others have explored visually-conditioned language generation [17, 114, 119, 124, 132] but have not yet shown good performance in low-data regimes.

We introduce *Flamingo*, a Visual Language Model (VLM) that sets a new state of the art in few-shot learning on a wide range of open-ended vision and language tasks, simply by being prompted with a few input/output examples, as illustrated in Figure 1. Of the 16 tasks we consider, *Flamingo* also surpasses the fine-tuned state of the art on 6 tasks, despite using orders of magnitude less task-specific training data (see Figure 2). To achieve this, Flamingo takes inspiration from recent work on large language models (LMs) which are good few-shot learners [11, 18, 42, 86]. A single large LM can achieve strong performance on many tasks using only its text interface: a few examples of a task are provided to the model as a prompt, along with a query input, and the model generates a continuation to produce a predicted output for that query. We show that the same can be done for image and video understanding tasks such as classification, captioning, or question-answering: these can be cast as text prediction problems with visual input conditioning. The difference from a LM is that the model must be able to ingest a multimodal prompt containing images and/or videos interleaved with text. Flamingo models have this capability—they are visually-conditioned autoregressive text generation models able to ingest a sequence of text tokens interleaved with images and/or videos, and produce text as output. Flamingo models leverage two complementary pre-trained and frozen models: a vision model which can “perceive” visual scenes and a large LM which performs a basic form of reasoning. Novel architecture components are added in between these models to connect them in a way that preserves the knowledge they have accumulated during computationally intensive pre-training. Flamingo models are also able to ingest high-resolution images or videos thanks to a Perceiver-based [48] architecture that can produce a small fixed number of visual tokens per image/video, given a large and variable number of visual input features.

A crucial aspect for the performance of large LMs is that they are trained on a large amount of text data. This training provides general-purpose generation capabilities that allows these LMs to perform well when prompted with task examples. Similarly, we demonstrate that the way we train the Flamingo models is crucial for their final performance. They are trained on a carefully chosen

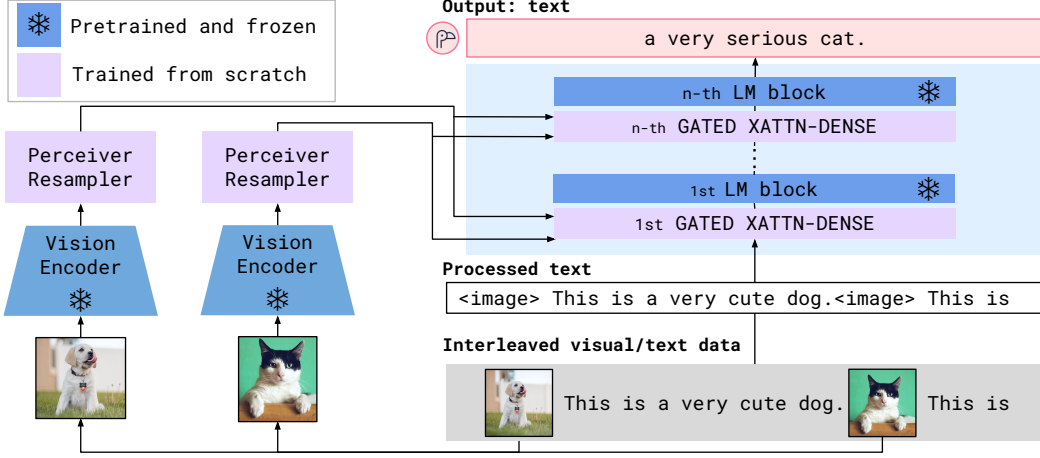


Figure 3: **Flamingo architecture overview.** Flamingo is a family of visual language models (VLMs) that take as input visual data interleaved with text and produce free-form text as output.

mixture of complementary large-scale multimodal data coming only from the web, *without using any data annotated for machine learning purposes*. After this training, a Flamingo model can be directly adapted to vision tasks via simple few-shot learning without any task-specific tuning.

Contributions. In summary, our contributions are the following: **(i)** We introduce the Flamingo family of VLMs which can perform various multimodal tasks (such as captioning, visual dialogue, or visual question-answering) from only a few input/output examples. Thanks to architectural innovations, the Flamingo models can efficiently accept arbitrarily interleaved visual data and text as input and generate text in an open-ended manner. **(ii)** We quantitatively evaluate how Flamingo models can be adapted to various tasks via few-shot learning. We notably reserve a large set of held-out benchmarks which have not been used for validation of any design decisions or hyperparameters of the approach. We use these to estimate unbiased few-shot performance. **(iii)** *Flamingo* sets a new state of the art in few-shot learning on a wide array of 16 multimodal language and image/video understanding tasks. On 6 of these 16 tasks, *Flamingo* also outperforms the fine-tuned state of the art despite using only 32 task-specific examples, around 1000 times less task-specific training data than the current state of the art. With a larger annotation budget, *Flamingo* can also be effectively fine-tuned to set a new state of the art on five additional challenging benchmarks: VQAv2, VATEX, VizWiz, MSRVTTQA, and HatefulMemes.

2 Approach

This section describes Flamingo: a visual language model that accepts text interleaved with images/videos as input and outputs free-form text. The key architectural components shown in Figure 3 are chosen to leverage pretrained vision and language models and bridge them effectively. First, the Perceiver Resampler (Section 2.1) receives spatio-temporal features from the Vision Encoder (obtained from either an image or a video) and outputs a fixed number of visual tokens. Second, these visual tokens are used to condition the frozen LM using freshly initialised cross-attention layers (Section 2.2) that are interleaved between the pretrained LM layers. These new layers offer an expressive way for the LM to incorporate visual information for the next-token prediction task. Flamingo models the likelihood of text y conditioned on interleaved images and videos x as follows:

$$p(y|x) = \prod_{\ell=1}^L p(y_\ell|y_{<\ell}, x_{\leq \ell}), \quad (1)$$

where y_ℓ is the ℓ -th language token of the input text, $y_{<\ell}$ is the set of preceding tokens, $x_{\leq \ell}$ is the set of images/videos preceding token y_ℓ in the interleaved sequence and p is parametrized by a Flamingo model. The ability to handle interleaved text and visual sequences (Section 2.3) makes it natural to use Flamingo models for in-context few-shot learning, analogously to GPT-3 with few-shot text prompting. The model is trained on a diverse mixture of datasets as described in Section 2.4.

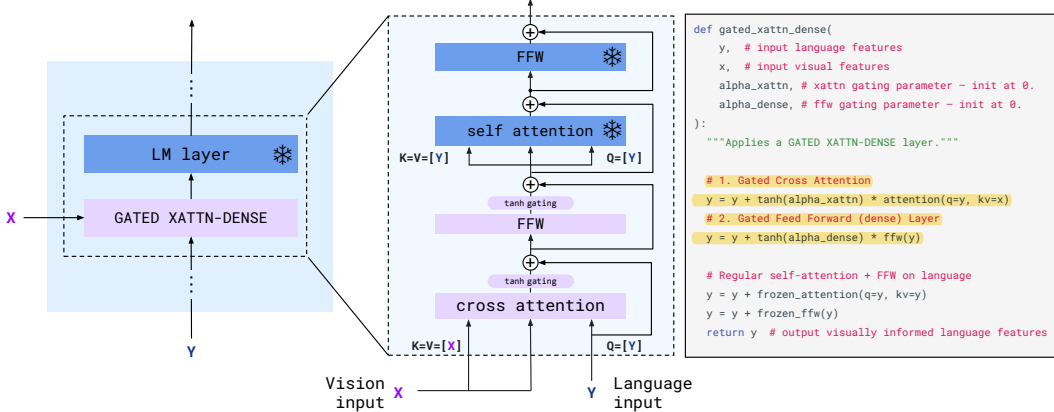


Figure 4: **GATED XATTN-DENSE layers.** To condition the LM on visual inputs, we insert new cross-attention layers between existing pretrained and frozen LM layers. The keys and values in these layers are obtained from the vision features while the queries are derived from the language inputs. They are followed by dense feed-forward layers. These layers are *gated* so that the LM is kept intact at initialization for improved stability and performance.

2.1 Visual processing and the Perceiver Resampler

Vision Encoder: from pixels to features. Our vision encoder is a pretrained and frozen Normalizer-Free ResNet (NFNet) [10] – we use the F6 model. We pretrain the vision encoder using a contrastive objective on our datasets of image and text pairs, using the two-term contrastive loss from Radford et al. [85]. We use the output of the final stage, a 2D spatial grid of features that is flattened to a 1D sequence. For video inputs, frames are sampled at 1 FPS and encoded independently to obtain a 3D spatio-temporal grid of features to which learned temporal embeddings are added. Features are then flattened to 1D before being fed to the Perceiver Resampler. More details on the contrastive model training and performance are given in Appendix B.1.3 and Appendix B.3.2, respectively.

Perceiver Resampler: from varying-size large feature maps to few visual tokens. This module connects the vision encoder to the frozen language model as shown in Figure 3. It takes as input a variable number of image or video features from the vision encoder and produces a fixed number of visual outputs (64), reducing the computational complexity of the vision-text cross-attention. Similar to Perceiver [48] and DETR [13], we learn a predefined number of latent input queries which are fed to a Transformer and cross-attend to the visual features. We show in our ablation studies (Section 3.3) that using such a vision-language resampler module outperforms a plain Transformer and an MLP. We provide an illustration, more architectural details, and pseudo-code in Appendix A.1.1.

2.2 Conditioning frozen language models on visual representations

Text generation is performed by a Transformer decoder, conditioned on the visual representations produced by the Perceiver Resampler. We interleave pretrained and frozen text-only LM blocks with blocks trained from scratch that cross-attend to the visual output from the Perceiver Resampler.

Interleaving new GATED XATTN-DENSE layers within a frozen pretrained LM. We freeze the pretrained LM blocks, and insert *gated cross-attention dense* blocks (Figure 4) between the original layers, trained from scratch. To ensure that at initialization, the conditioned model yields the same results as the original language model, we use a tanh-gating mechanism [41]. This multiplies the output of a newly added layer by $\tanh(\alpha)$ before adding it to the input representation from the residual connection, where α is a layer-specific learnable scalar initialized to 0 [4]. Thus, at initialization, the model output matches that of the pretrained LM, improving training stability and final performance. In our ablation studies (Section 3.3), we compare the proposed GATED XATTN-DENSE layers against recent alternatives [22, 68] and explore the effect of how frequently these additional layers are inserted to trade off between efficiency and expressivity. See Appendix A.1.2 for more details.

Varying model sizes. We perform experiments across three models sizes, building on the 1.4B, 7B, and 70B parameter Chinchilla models [42]; calling them respectively *Flamingo-3B*, *Flamingo-9B* and

Flamingo-80B. For brevity, we refer to the last as *Flamingo* throughout the paper. While increasing the parameter count of the frozen LM and the trainable vision-text GATED XATTN-DENSE modules, we maintain a fixed-size frozen vision encoder and trainable Perceiver Resampler across the different models (small relative to the full model size). See Appendix B.1.1 for further details.

2.3 Multi-visual input support: per-image/video attention masking

The image-causal modelling introduced in Equation (1) is obtained by masking the full text-to-image cross-attention matrix, limiting which visual tokens the model sees at each text token. At a given text token, the model attends to the visual tokens of the image that appeared just before it in the interleaved sequence, rather than to all previous images (formalized and illustrated in Appendix A.1.3). Though the model only *directly* attends to a single image at a time, the dependency on all previous images remains via self-attention in the LM. This single-image cross-attention scheme importantly allows the model to seamlessly generalise to any number of visual inputs, regardless of how many are used during training. In particular, we use only up to 5 images per sequence when training on our interleaved datasets, yet our model is able to benefit from sequences of up to 32 pairs (or “shots”) of images/videos and corresponding texts during evaluation. We show in Section 3.3 that this scheme is more effective than allowing the model to cross-attend to all previous images directly.

2.4 Training on a mixture of vision and language datasets

We train the Flamingo models on a mixture of three kinds of datasets, all scraped from the web: an interleaved image and text dataset derived from webpages, image-text pairs, and video-text pairs.

M3W: Interleaved image and text dataset. The few-shot capabilities of Flamingo models rely on training on interleaved text and image data. For this purpose, we collect the *MultiModal MassiveWeb (M3W)* dataset. We extract both text and images from the HTML of approximately 43 million webpages, determining the positions of images relative to the text based on the relative positions of the text and image elements in the Document Object Model (DOM). An example is then constructed by inserting `<image>` tags in plain text at the locations of the images on the page, and inserting a special `<EOC>` (*end of chunk*) token (added to the vocabulary and learnt) prior to any image and at the end of the document. From each document, we sample a random subsequence of $L = 256$ tokens and take up to the first $N = 5$ images included in the sampled sequence. Further images are discarded in order to save compute. More details are provided in Appendix A.3.

Pairs of image/video and text. For our image and text pairs we first leverage the ALIGN [50] dataset, composed of 1.8 billion images paired with alt-text. To complement this dataset, we collect our own dataset of image and text pairs targeting better quality and longer descriptions: LTIP (Long Text & Image Pairs) which consists of 312 million image and text pairs. We also collect a similar dataset but with videos instead of still images: VTP (Video & Text Pairs) consists of 27 million short videos (approximately 22 seconds on average) paired with sentence descriptions. We align the syntax of paired datasets with the syntax of M3W by prepending `<image>` and appending `<EOC>` to each training caption (see Appendix A.3.3 for details).

Multi-objective training and optimisation strategy. We train our models by minimizing a weighted sum of per-dataset expected negative log-likelihoods of text, given the visual inputs:

$$\sum_{m=1}^M \lambda_m \cdot \mathbb{E}_{(x,y) \sim \mathcal{D}_m} \left[- \sum_{\ell=1}^L \log p(y_\ell | y_{<\ell}, x_{\leq \ell}) \right], \quad (2)$$

where \mathcal{D}_m and λ_m are the m -th dataset and its weighting, respectively. Tuning the per-dataset weights λ_m is key to performance. We accumulate gradients over all datasets, which we found outperforms a “round-robin” approach [17]. We provide further training details and ablations in Appendix B.1.2.

2.5 Task adaptation with few-shot in-context learning

Once Flamingo is trained, we use it to tackle a visual task by conditioning it on a multimodal interleaved prompt. We evaluate the ability of our models to rapidly adapt to new tasks using **in-context learning**, analogously to GPT-3 [11], by interleaving support example pairs in the form of $(image, text)$ or $(video, text)$, followed by the query visual input, to build a prompt (details in Appendix A.2). We perform **open-ended** evaluations using beam search for decoding, and **close-ended**

Method	FT	Shot	OKVQA (I)	VQAv2 (I)	COCO (I)	MSVDQA (V)	VATEX (V)	VizWiz (I)	Flick30K (I)	MSRVTTQA (V)	iVQA (V)	STAR (V)	YouCook2 (V)	VisDial (I)	TextVQA (I)	NextQA (I)	HatefulMemes (I)	RareAct (V)
Zero/Few shot SOTA	\times	(X)	[34]	[114]	[124]	[58]	-	-	-	[58]	[135]	[143]	[79]	-	-	[85]	[85]	
		(16)	43.3	38.2	32.2	35.2	(0)	(0)	(0)	19.2	12.2	39.4	11.6	(0)	(0)	66.1	40.7	
<i>Flamingo</i> -3B	\times	0	41.2	49.2	73.0	27.5	40.1	28.9	60.6	11.0	32.7	39.6	46.1	30.1	21.3	53.7	58.4	
		4	43.3	53.2	85.0	33.0	50.0	34.0	72.0	14.9	35.7	64.6	41.3	47.3	32.7	22.4	53.6	-
	\times	32	45.9	57.1	99.0	42.6	59.2	45.5	71.2	25.6	37.7	76.7	41.6	47.3	30.6	26.1	56.3	-
<i>Flamingo</i> -9B	\times	0	44.7	51.8	79.4	30.2	39.5	28.8	61.5	13.7	35.2	55.0	41.8	48.0	31.8	23.0	57.0	57.9
		4	49.3	56.3	93.1	36.2	51.7	34.9	72.6	18.2	37.7	70.8	42.8	50.4	33.6	24.7	62.7	-
	\times	32	51.0	60.4	106.3	47.2	57.4	44.0	72.8	29.4	40.7	77.3	41.2	50.4	32.6	28.4	63.5	-
<i>Flamingo</i>	\times	0	50.6	56.3	84.3	35.6	46.7	31.6	67.2	17.4	40.7	60.1	39.7	52.0	35.0	26.7	46.4	60.8
		4	57.4	63.1	103.2	41.7	56.0	39.6	75.1	23.9	44.1	74.5	42.4	55.6	36.5	30.8	68.6	-
	\times	32	57.8	67.6	113.8	52.3	65.1	49.8	75.4	31.0	45.3	86.8	42.2	55.6	37.9	33.5	70.0	-
Pretrained FT SOTA	\checkmark	(X)	54.4 (10K) (444K)	80.2 [34] [140]	143.3 [124]	47.9 [28]	76.3 [153]	57.2 [65]	67.4 [150]	46.8 [51]	35.4 [135]	138.7 [132]	36.7 [128]	75.2 [79]	54.7 [137]	25.2 [129]	79.1 [62]	-
		(10K)	(444K)	(500K)	(27K)	(500K)	(20K)	(30K)	(130K)	(6K)	(10K)	(46K)	(123K)	(20K)	(38K)	(9K)	-	

Table 1: **Comparison to the state of the art.** A single Flamingo model reaches the state of the art on a wide array of image (I) and video (V) understanding tasks with few-shot learning, significantly outperforming previous best zero- and few-shot methods with as few as four examples. More importantly, using only 32 examples and without adapting any model weights, Flamingo *outperforms* the current best methods – fine-tuned on thousands of annotated examples – on seven tasks. Best few-shot numbers are in **bold**, best numbers overall are underlined.

evaluations using our model’s log-likelihood to score each possible answer. We explore **zero-shot generalization** by prompting the model with two text-only examples from the task, with no corresponding images. Evaluation hyperparameters and additional details are given in Appendix B.1.5.

3 Experiments

Our goal is to develop models that can rapidly adapt to diverse and challenging tasks. For this, we consider a wide array of 16 popular multimodal image/video and language benchmarks. In order to validate model design decisions during the course of the project, 5 of these benchmarks were used as part of our development (DEV) set: COCO, OKVQA, VQAv2, MSVDQA and VATEX. Performance estimates on the DEV benchmarks may be biased, as a result of model selection. We note that this is also the case for prior work which makes use of similar benchmarks to validate and ablate design decisions. To account for this, we report performance on an additional set of 11 benchmarks, spanning captioning, video question-answering, as well as some less commonly explored capabilities such as visual dialogue and multi-choice question-answering tasks. The evaluation benchmarks are described in Appendix B.1.4. We keep all evaluation hyperparameters fixed across all benchmarks. Depending on the task, we use four few-shot prompt templates we describe in more detail in Appendix B.1.5. We emphasize that *we do not validate any design decisions on these 11 benchmarks* and use them solely to estimate unbiased few-shot learning performance of our models.

Concretely, estimating few-shot learning performance of a model involves prompting it with a set of *support* samples and evaluating it on a set of *query* samples. For the DEV benchmarks that are used both to validate design decisions and hyperparameters, as well as to report final performance, we therefore use four subsets: *validation support*, *validation query*, *test support* and *test query*. For other benchmarks, we need only the latter two. We report in Appendix B.1.4 how we form these subsets.

We report the results of the Flamingo models on few-shot learning in Section 3.1. Section 3.2 gives Flamingo fine-tuned results. An ablation study is given in Section 3.3. Appendix B.2 provides more results including Flamingo’s performance on the ImageNet and Kinetics700 classification tasks, and on our contrastive model’s performance. Appendix C includes additional qualitative results.

3.1 Few-shot learning on vision-language tasks

Few-shot results. Results are given in Table 1. Flamingo outperforms by a large margin *all* previous zero-shot or few-shot methods on the 16 benchmarks considered. This is achieved with as few as four examples per task, demonstrating practical and efficient adaptation of vision models to new tasks. More importantly, Flamingo is often competitive with state-of-the-art methods additionally fine-tuned on up to hundreds of thousands of annotated examples. On six tasks, Flamingo even outperforms the fine-tuned SotA despite using a *single* set of model weights and only 32 task-specific examples.

Method	VQAv2		COCO test	VATEX test	VizWiz		MSRVTTQA test	VisDial		YouCook2 valid	TextVQA valid	TextVQA test-std	HatefulMemes test seen
	test-dev	test-std			test-dev	test-std		valid	test-std				
32 shots	67.6	-	113.8	65.1	49.8	-	31.0	56.8	-	86.8	36.0	-	70.0
Fine-tuned	82.0	82.1	138.1	84.2	65.7	65.4	47.4	61.8	59.7	118.6	57.1	54.1	86.6
SotA	81.3 [†]	81.3 [†]	149.6[†]	81.4 [†]	57.2 [†]	60.6 [†]	46.8	75.2	75.4[†]	138.7	54.7	73.7	84.6 [†]
	[133]	[133]	[119]	[153]	[65]	[65]	[51]	[79]	[123]	[132]	[137]	[84]	[152]

Table 2: **Comparison to SotA when fine-tuning Flamingo.** We fine-tune *Flamingo* on all nine tasks where *Flamingo* does not achieve SotA with few-shot learning. *Flamingo* sets a new SotA on five of them, outperforming methods (marked with [†]) that use tricks such as model ensembling or domain-specific metric optimisation (e.g., CIDEr optimisation).

Ablated setting	Flamingo-3B original value	Changed value	Param. count ↓	Step time ↓	COCO CIDEr↑	OKVQA top1↑	VQAv2 top1↑	MSVDQA top1↑	VATEX CIDEr↑	Overall score↑	
Flamingo-3B model											
(i) Training data	All data	w/o Video-Text pairs	3.2B	1.74s	86.5	42.1	55.8	36.3	53.4	70.7	
		w/o Image-Text pairs	3.2B	0.95s	66.3	39.2	51.6	32.0	41.6	67.3	
		Image-Text pairs → LAION	3.2B	1.74s	79.5	41.4	53.5	33.9	47.6	60.9	
		w/o M3W	3.2B	1.02s	54.1	36.5	52.7	31.4	23.5	66.4	
(ii) Optimisation	Accumulation	Round Robin	3.2B	1.68s	76.1	39.8	52.1	33.2	40.8	62.9	
(iii)	Tanh gating	✓	✗	3.2B	1.74s	78.4	40.5	52.9	35.9	47.5	66.5
(iv)	Cross-attention architecture	GATED XATTN-DENSE	VANILLA XATTN GRAFTING	2.4B 3.3B	1.16s 1.74s	80.6 79.2	41.5 36.1	53.4 50.8	32.9 32.2	50.7 47.8	66.9 63.1
(v)	Cross-attention frequency	Every	Single in middle Every 4th Every 2nd	2.0B 2.3B 2.6B	0.87s 1.02s 1.24s	71.5 82.3 83.7	38.1 42.7 41.0	50.2 55.1 55.8	29.1 34.6 34.5	42.3 50.8 49.7	59.8 68.8 68.2
(vi)	Resampler	Perceiver	MLP Transformer	3.2B 3.2B	1.85s 1.81s	78.6 83.2	42.2 41.7	54.7 55.6	35.2 31.5	44.7 48.3	66.6 66.7
(vii)	Vision encoder	NFNet-F6	CLIP ViT-L/14 NFNet-F0	3.1B 2.9B	1.58s 1.45s	76.5 73.8	41.6 40.5	53.4 52.8	33.2 31.1	44.5 42.9	64.9 62.7
(viii)	Freezing LM	✓	✗ (random init) ✗ (pretrained)	3.2B 3.2B	2.42s 2.42s	74.8 81.2	31.5 33.7	45.6 47.4	26.9 31.0	50.1 53.9	57.8 62.7

Table 3: **Ablation studies.** Each row should be compared to the baseline Flamingo run (top row). Step time measures the time spent to perform gradient updates on all training datasets.

Finally, despite having only used the DEV benchmarks for design decisions, our results generalize well to the other benchmarks, confirming the generality of our approach.

Scaling with respect to parameters and shots. As shown in Figure 2, the larger the model, the better the few-shot performance, similar to GPT-3 [11]. The performance also improves with the number of shots. We further find that the largest model better exploits larger numbers of shots. Interestingly, even though our Flamingo models were trained with sequences limited to only 5 images on *M3W*, they are still able to benefit from up to 32 images or videos during inference. This demonstrates the flexibility of the Flamingo architecture for processing a variable number of videos or images.

3.2 Fine-tuning Flamingo as a pretrained vision-language model

While not the main focus of our work, we verify that when given more data, Flamingo models can be adapted to a task by fine-tuning their weights. In Table 2, we explore fine-tuning our largest model, *Flamingo*, for a given task with no limit on the annotation budget. In short, we do so by fine-tuning the model on a short schedule with a small learning rate by additionally unfreezing the vision backbone to accommodate a higher input resolution (details in Appendix B.2.2). We find that we can improve results over our previously presented in-context few-shot learning results, setting a new state of the art on five additional tasks: VQAv2, VATEX, VizWiz, MSRVTTQA, and HatefulMemes.

3.3 Ablation studies

In Table 3, we report our ablation results using Flamingo-3B on the validation subsets of the five DEV benchmarks with 4 shots. Note that we use smaller batch sizes and a shorter training schedule compared to the final models. The **Overall score** is obtained by dividing each benchmark score by its state-of-the-art (SotA) performance from Table 1 and averaging the results. More details and results are given in Appendix B.3 and Table 10.

Importance of the training data mixture. As shown in row (i), getting the right training data plays a crucial role. In fact, removing the interleaved image-text dataset *M3W* leads to a *decrease of more than 17%* in performance while removing the conventional paired image-text pairs also decreases

performance (by 9.8%), demonstrating the need for different types of datasets. Moreover, removing our paired video-text dataset negatively affects performance on all video tasks. We ablate replacing our image-text pairs (ITP) by the publicly available LAION-400M dataset [96], which leads to a slight degradation in performance. We show in row (ii) the importance of our gradient accumulation strategy compared to using round-robin updates [17].

Visual conditioning of the frozen LM. We ablate the use of the 0-initialized tanh gating when merging the cross-attention output to the frozen LM output in row (iii). Without it, we see a drop of 4.2% in our overall score. Moreover, we have noticed that disabling the 0-initialized tanh gating leads to training instabilities. Next, we ablate different conditioning architectures in row (iv). VANILLA XATTN, refers to the vanilla cross-attention from the original Transformer decoder [115]. In the GRAFTING approach from [68], the frozen LM is used as is with no additional layers inserted, and a stack of interleaved self-attention and cross-attention layers that take the frozen LM output are learnt from scratch. Overall, we show that our GATED XATTN-DENSE conditioning approach works best.

Compute/Memory vs. performance trade-offs. In row (v), we ablate the frequency at which we add new GATED XATTN-DENSE blocks. Although adding them at every layer is better, it significantly increases the number of trainable parameters and time complexity of the model. Notably, inserting them every fourth block accelerates training by 66% while only decreasing the overall score by 1.9%. In light of this trade-off, we maximize the number of added layers under hardware constraints and add a GATED XATTN-DENSE every fourth layer for *Flamingo*-9B and every seventh for *Flamingo*-80B. We further compare in row (vi) the Perceiver Resampler to a MLP and a vanilla Transformer given a parameter budget. Both underperform the Perceiver Resampler while also being slower.

Vision encoder. In row (vii), we compare our NFNet-F6 vision encoder pretrained with contrastive learning (details in Appendix B.1.3) to the publicly available CLIP ViT-L/14 [85] model trained at 224 resolution. Our NFNet-F6 has a +5.8% advantage over the CLIP ViT-L/14 and +8.0% over a smaller NFNet-F0 encoder, which highlights the importance of using a strong vision backbone.

Freezing LM components prevents catastrophic forgetting. We verify the importance of freezing the LM layers at training in row (viii). If trained from scratch, we observe a large performance decrease of –12.9%. Interestingly, fine-tuning our pretrained LM also leads to a drop in performance of –8.0%. This indicates an instance of “catastrophic forgetting” [71], in which the model progressively forgets its pretraining while training on a new objective. In our setting, freezing the language model is a better alternative to training with the pre-training dataset (MassiveText) in the mixture.

4 Related work

Language modelling and few-shot adaptation. Language modelling has recently made substantial progress following the introduction of Transformers [115]. The paradigm of first pretraining on a vast amount of data followed by an adaptation on a downstream task has become standard [11, 23, 32, 44, 52, 75, 87, 108]. In this work, we build on the 70B Chinchilla language model [42] as the base LM for *Flamingo*. Numerous works have explored techniques to adapt language models to novel tasks using a few examples. These include adding small adapter modules [43], fine-tuning a small part of the LM [141], showing in-context examples in the prompt [11], or optimizing the prompt [56, 60] through gradient descent. In this paper, we take inspiration from the in-context [11] few-shot learning technique instead of more involved few-shot learning approaches based on metric learning [24, 103, 112, 117] or meta-learning [6, 7, 27, 31, 91, 155].

When language meets vision. These LM breakthroughs have been influential for vision-language modelling. In particular, BERT [23] inspired a large body of vision-language work [16, 28, 29, 38, 59, 61, 66, 101, 106, 107, 109, 118, 121, 142, 143, 151]. We differ from these approaches as Flamingo models do not require fine-tuning on new tasks. Another family of vision-language models is based on contrastive learning [2, 5, 49, 50, 57, 74, 82, 85, 138, 140, 146]. Flamingo differs from contrastive models as it can generate text, although we build and rely upon them for our vision encoder. Similar to our work are VLMs able to generate text in an autoregressive manner [19, 25, 45, 67, 116]. Concurrent works [17, 58, 119, 124, 154] also propose to formulate numerous vision tasks as text generation problems. Building on top of powerful pretrained language models has been explored in several recent works. One recent line of work [26, 68, 78, 114, 136, 144] proposes to freeze the pretrained LM weights to prevent catastrophic forgetting [71]. We follow this idea by freezing the

Chinchilla LM layers [42] and adding learnable layers within the frozen LM. We differ from prior work by introducing the first LM that can ingest arbitrarily interleaved images, videos, and text.

Web-scale vision and language training datasets. Manually annotated vision and language datasets are costly to obtain and thus relatively small (10k-100k) in scale [3, 15, 69, 122, 129, 139]. To alleviate this lack of data, numerous works [14, 50, 98, 110] automatically scrape readily available paired vision-text data. In addition to such paired data, we show the importance of also training on entire multimodal webpages containing interleaved images and text as a single sequence. Concurrent work CM3 [1] proposes to generate HTML markup from pages, while we simplify the text prediction task by only generating plain text. We emphasize few-shot learning and vision tasks while CM3 [1] primarily evaluates on language-only benchmarks in a zero-shot or fine-tuned setup.

5 Discussion

Limitations. First, our models build on pretrained LMs, and as a side effect, directly inherit their weaknesses. For example, LM priors are generally helpful, but may play a role in occasional hallucinations and ungrounded guesses. Furthermore, LMs generalise poorly to sequences longer than the training ones. They also suffer from poor sample efficiency during training. Addressing these issues can accelerate progress in the field and enhance the abilities of VLMs like Flamingo.

Second, the classification performance of Flamingo lags behind that of state-of-the-art contrastive models [82, 85]. These models directly optimize for text-image retrieval, of which classification is a special case. In contrast, our models handle a wider range of tasks, such as open-ended ones. A unified approach to achieve the best of both worlds is an important research direction.

Third, in-context learning has significant advantages over gradient-based few-shot learning methods, but also suffers from drawbacks depending on the characteristics of the application at hand. We demonstrate the effectiveness of in-context learning when access is limited to only a few dozen examples. In-context learning also enables simple deployment, requiring only inference, generally with no hyperparameter tuning needed. However, in-context learning is known to be highly sensitive to various aspects of the demonstrations [80, 148], and its inference compute cost and absolute performance scale poorly with the number of shots beyond this low-data regime. There may be opportunities to combine few-shot learning methods to leverage their complementary benefits. We discuss the limitations of our work in more depth in Appendix D.1.

Societal impacts. In terms of societal impacts, *Flamingo* offers a number of benefits while carrying some risks. Its ability to rapidly adapt to a broad range of tasks have the potential to enable non-expert users to obtain good performance in data-starved regimes, lowering the barriers to both beneficial and malicious applications. *Flamingo* is exposed to the same risks as large language models, such as outputting offensive language, propagating social biases and stereotypes, as well as leaking private information [42, 126]. Its ability to additionally handle visual inputs poses specific risks such as gender and racial biases relating to the contents of the input images, similar to a number of visual recognition systems [12, 21, 37, 97, 147]. We refer the reader to Appendix D.2 for a more extensive discussion of the societal impacts of our work, both positive and negative; as well as mitigation strategies and early investigations of risks relating to racial or gender bias and toxic outputs. Finally we note that, following prior work focusing on language models [72, 81, 111], the few-shot capabilities of Flamingo could be useful for mitigating such risks.

Conclusion. We proposed Flamingo, a general-purpose family of models that can be applied to image and video tasks with minimal task-specific training data. We also qualitatively explored interactive abilities of *Flamingo* such as “chatting” with the model, demonstrating flexibility beyond traditional vision benchmarks. Our results suggest that connecting pre-trained large language models with powerful visual models is an important step towards general-purpose visual understanding.

Acknowledgments and Disclosure of Funding. This research was funded by DeepMind. We would like to thank many colleagues for useful discussions, suggestions, feedback, and advice, including: Samuel Albanie, Relja Arandjelović, Kareem Ayoub, Lorrayne Bennett, Adria Recasens Conti-nente, Tom Eccles, Nando de Freitas, Sander Dieleman, Conor Durkan, Aleksa Gordić, Raia Hadsell, Will Hawkins, Lisa Anne Hendricks, Felix Hill, Jordan Hoffmann, Geoffrey Irving, Drew Jaegle, Koray Kavukcuoglu, Agustin Dal Lago, Mateusz Malinowski, Soňa Mokrá, Gaby Pearl, Toby Pohlen, Jack Rae, Laurent Sifre, Francis Song, Maria Tsimpoukelli, Gregory Wayne, and Boxi Wu.

References

- [1] Armen Aghajanyan, Bernie Huang, Candace Ross, Vladimir Karpukhin, Hu Xu, Naman Goyal, Dmytro Okhonko, Mandar Joshi, Gargi Ghosh, Mike Lewis, and Luke Zettlemoyer. CM3: A causal masked multimodal model of the internet. *arXiv:2201.07520*, 2022.
- [2] Jean-Baptiste Alayrac, Adria Recasens, Rosalia Schneider, Relja Arandjelović, Jason Ramanpuram, Jeffrey De Fauw, Lucas Smaira, Sander Dieleman, and Andrew Zisserman. Self-supervised multimodal versatile networks. *Conference on Neural Information Processing Systems*, 2020.
- [3] Stanislaw Antol, Aishwarya Agrawal, Jiasen Lu, Margaret Mitchell, Dhruv Batra, C. Lawrence Zitnick, and Devi Parikh. VQA: Visual question answering. In *International Conference on Computer Vision*, 2015.
- [4] Thomas Bachlechner, Bodhisattwa Prasad Majumder, Henry Mao, Gary Cottrell, and Julian McAuley. ReZero is all you need: Fast convergence at large depth. In *Uncertainty in Artificial Intelligence*, 2021.
- [5] Max Bain, Arsha Nagrani, Gü̈l Varol, and Andrew Zisserman. Frozen in time: A joint video and image encoder for end-to-end retrieval. In *International Conference on Computer Vision*, 2021.
- [6] Luca Bertinetto, João F. Henriques, Jack Valmadre, Philip Torr, and Andrea Vedaldi. Learning feed-forward one-shot learners. *Conference on Neural Information Processing Systems*, 2016.
- [7] Luca Bertinetto, Joao F. Henriques, Philip H. S. Torr, and Andrea Vedaldi. Meta-learning with differentiable closed-form solvers. *arXiv:1805.08136*, 2018.
- [8] James Bradbury, Roy Frostig, Peter Hawkins, Matthew James Johnson, Chris Leary, Dougal Maclaurin, George Necula, Adam Paszke, Jake VanderPlas, Skye Wanderman-Milne, and Qiao Zhang. JAX: composable transformations of Python+NumPy programs, 2018. URL <http://github.com/google/jax>.
- [9] John S. Bridle. Probabilistic interpretation of feedforward classification network outputs, with relationships to statistical pattern recognition. In *Neurocomputing*, 1990.
- [10] Andrew Brock, Soham De, Samuel L. Smith, and Karen Simonyan. High-performance large-scale image recognition without normalization. *arXiv:2102.06171*, 2021.
- [11] Tom B. Brown, Benjamin Mann, Nick Ryder, Melanie Subbiah, Jared Kaplan, Prafulla Dhariwal, Arvind Neelakantan, Pranav Shyam, Girish Sastry, Amanda Askell, Sandhini Agarwal, Ariel Herbert-Voss, Gretchen Krueger, Tom Henighan, Rewon Child, Aditya Ramesh, Daniel M. Ziegler, Jeffrey Wu, Clemens Winter, Christopher Hesse, Mark Chen, Eric Sigler, Mateusz Litwin, Scott Gray, Benjamin Chess, Jack Clark, Christopher Berner, Sam McCandlish, Alec Radford, Ilya Sutskever, and Dario Amodei. Language models are few-shot learners. In *Conference on Neural Information Processing Systems*, 2020.
- [12] Joy Buolamwini and Timnit Gebru. Gender shades: Intersectional accuracy disparities in commercial gender classification. In *ACM Conference on Fairness, Accountability, and Transparency*, 2018.
- [13] Nicolas Carion, Francisco Massa, Gabriel Synnaeve, Nicolas Usunier, Alexander Kirillov, and Sergey Zagoruyko. End-to-end object detection with transformers. In *European Conference on Computer Vision*, 2020.
- [14] Soravit Changpinyo, Piyush Sharma, Nan Ding, and Radu Soricut. Conceptual 12M: Pushing web-scale image-text pre-training to recognize long-tail visual concepts. In *IEEE Computer Vision and Pattern Recognition*, 2021.
- [15] Xinlei Chen, Hao Fang, Tsung-Yi Lin, Ramakrishna Vedantam, Saurabh Gupta, Piotr Dollár, and C Lawrence Zitnick. Microsoft COCO captions: Data collection and evaluation server. *arXiv:1504.00325*, 2015.

- [16] Yen-Chun Chen, Linjie Li, Licheng Yu, Ahmed El Kholy, Faisal Ahmed, Zhe Gan, Yu Cheng, and Jingjing Liu. UNITER: Universal image-text representation learning. In *European Conference on Computer Vision*, 2020.
- [17] Jaemin Cho, Jie Lei, Hao Tan, and Mohit Bansal. Unifying vision-and-language tasks via text generation. In *International Conference on Machine Learning*, 2021.
- [18] Aakanksha Chowdhery, Sharan Narang, Jacob Devlin, Maarten Bosma, Gaurav Mishra, Adam Roberts, Paul Barham, Hyung Won Chung, Charles Sutton, Sebastian Gehrmann, Parker Schuh, Kensen Shi, Sasha Tsvyashchenko, Joshua Maynez, Abhishek Rao, Parker Barnes, Yi Tay, Noam Shazeer, Vinodkumar Prabhakaran, Emily Reif, Nan Du, Ben Hutchinson, Reiner Pope, James Bradbury, Jacob Austin, Michael Isard, Guy Gur-Ari, Pengcheng Yin, Toju Duke, Anselm Levskaya, Sanjay Ghemawat, Sunipa Dev, Henryk Michalewski, Xavier Garcia, Vedant Misra, Kevin Robinson, Liam Fedus, Denny Zhou, Daphne Ippolito, David Luan, Hyeontaek Lim, Barret Zoph, Alexander Spiridonov, Ryan Sepassi, David Dohan, Shivani Agrawal, Mark Omernick, Andrew M. Dai, Thanumalayan Sankaranarayana Pillai, Marie Pellat, Aitor Lewkowycz, Erica Moreira, Rewon Child, Oleksandr Polozov, Katherine Lee, Zongwei Zhou, Xuezhi Wang, Brennan Saeta, Mark Diaz, Orhan Firat, Michele Catasta, Jason Wei, Kathy Meier-Hellstern, Douglas Eck, Jeff Dean, Slav Petrov, and Noah Fiedel. PaLM: Scaling language modeling with pathways. *arXiv:2204.02311*, 2022.
- [19] Wenliang Dai, Lu Hou, Lifeng Shang, Xin Jiang, Qun Liu, and Pascale Fung. Enabling multimodal generation on clip via vision-language knowledge distillation. In *ACL Findings*, 2022.
- [20] Abhishek Das, Satwik Kottur, Khushi Gupta, Avi Singh, Deshraj Yadav, José MF Moura, Devi Parikh, and Dhruv Batra. Visual dialog. In *IEEE Computer Vision and Pattern Recognition*, 2017.
- [21] Terrance De Vries, Ishan Misra, Changhan Wang, and Laurens Van der Maaten. Does object recognition work for everyone? In *IEEE Computer Vision and Pattern Recognition*, 2019.
- [22] Karan Desai and Justin Johnson. VirTex: Learning visual representations from textual annotations. In *IEEE Computer Vision and Pattern Recognition*, 2021.
- [23] Jacob Devlin, Ming-Wei Chang, Kenton Lee, and Kristina Toutanova. BERT: Pre-training of deep bidirectional transformers for language understanding. *arXiv:1810.04805*, 2018.
- [24] Carl Doersch, Ankush Gupta, and Andrew Zisserman. CrossTransformers: spatially-aware few-shot transfer. *Conference on Neural Information Processing Systems*, 2020.
- [25] Jeffrey Donahue, Lisa Anne Hendricks, Sergio Guadarrama, Marcus Rohrbach, Subhashini Venugopalan, Kate Saenko, and Trevor Darrell. Long-term recurrent convolutional networks for visual recognition and description. In *IEEE Computer Vision and Pattern Recognition*, 2015.
- [26] Constantin Eichenberg, Sidney Black, Samuel Weinbach, Letitia Parcalabescu, and Anette Frank. MAGMA—multimodal augmentation of generative models through adapter-based finetuning. *arXiv:2112.05253*, 2021.
- [27] Chelsea Finn, Pieter Abbeel, and Sergey Levine. Model-agnostic meta-learning for fast adaptation of deep networks. In *International Conference on Machine Learning*, 2017.
- [28] Tsu-Jui Fu, Linjie Li, Zhe Gan, Kevin Lin, William Yang Wang, Lijuan Wang, and Zicheng Liu. VIOLET: End-to-end video-language transformers with masked visual-token modeling. *arXiv:2111.12681*, 2021.
- [29] Zhe Gan, Yen-Chun Chen, Linjie Li, Chen Zhu, Yu Cheng, and Jingjing Liu. Large-scale adversarial training for vision-and-language representation learning. In *Conference on Neural Information Processing Systems*, 2020.
- [30] Timnit Gebru, Jamie Morgenstern, Briana Vecchione, Jennifer Wortman Vaughan, Hanna Wallach, Hal Daumé III, and Kate Crawford. Datasheets for datasets. *Communications of the ACM*, 2021.

- [31] Jonathan Gordon, John Bronskill, Matthias Bauer, Sebastian Nowozin, and Richard E. Turner. Meta-learning probabilistic inference for prediction. *arXiv:1805.09921*, 2018.
- [32] Alex Graves. Generating sequences with recurrent neural networks. *arXiv:1308.0850*, 2013.
- [33] Thomas L. Griffiths, Frederick Callaway, Michael B. Chang, Erin Grant, Paul M. Krueger, and Falk Lieder. Doing more with less: meta-reasoning and meta-learning in humans and machines. *Current Opinion in Behavioral Sciences*, 2019.
- [34] Liangke Gui, Borui Wang, Qiuyuan Huang, Alex Hauptmann, Yonatan Bisk, and Jianfeng Gao. KAT: A knowledge augmented transformer for vision-and-language. *arXiv:2112.08614*, 2021.
- [35] Danna Gurari, Qing Li, Abigale J. Stangl, Anhong Guo, Chi Lin, Kristen Grauman, Jiebo Luo, and Jeffrey P. Bigham. VizWiz grand challenge: Answering visual questions from blind people. In *IEEE Computer Vision and Pattern Recognition*, 2018.
- [36] Adi Haviv, Ori Ram, Ofir Press, Peter Izsak, and Omer Levy. Transformer language models without positional encodings still learn positional information. *arXiv:2203.16634*, 2022.
- [37] Lisa Anne Hendricks, Kaylee Burns, Kate Saenko, Trevor Darrell, and Anna Rohrbach. Women also snowboard: Overcoming bias in captioning models. In *European Conference on Computer Vision*, 2018.
- [38] Lisa Anne Hendricks, John Mellor, Rosalia Schneider, Jean-Baptiste Alayrac, and Aida Nematzadeh. Decoupling the role of data, attention, and losses in multimodal transformers. *Annual Meeting of the Association for Computational Linguistics*, 2021.
- [39] Dan Hendrycks and Kevin Gimpel. Gaussian error linear units (GELUs). *arXiv:1606.08415*, 2016.
- [40] Tom Hennigan, Trevor Cai, Tamara Norman, and Igor Babuschkin. Haiku: Sonnet for JAX, 2020. URL <http://github.com/deepmind/dm-haiku>.
- [41] Sepp Hochreiter and Jürgen Schmidhuber. Long short-term memory. *Neural Computation*, 1997.
- [42] Jordan Hoffmann, Sebastian Borgeaud, Arthur Mensch, Elena Buchatskaya, Trevor Cai, Eliza Rutherford, Diego de Las Casas, Lisa Anne Hendricks, Johannes Welbl, Aidan Clark, Eric Noland, Tom Hennigan, Katie Millican, George van den Driessche, Bogdan Damoc, Aurelia Guy, Simon Osindero, Karen Simonyan, Erich Elsen, Jack W. Rae, Oriol Vinyals, and Laurent Sifre. Training compute-optimal large language models. *arXiv:2203.15556*, 2022.
- [43] Neil Houlsby, Andrei Giurgiu, Stanislaw Jastrzebski, Bruna Morrone, Quentin De Laroussilhe, Andrea Gesmundo, Mona Attariyan, and Sylvain Gelly. Parameter-efficient transfer learning for NLP. In *International Conference on Machine Learning*, 2019.
- [44] Jeremy Howard and Sebastian Ruder. Universal language model fine-tuning for text classification. *arXiv:1801.06146*, 2018.
- [45] Xiaowei Hu, Zhe Gan, Jianfeng Wang, Zhengyuan Yang, Zicheng Liu, Yumao Lu, and Lijuan Wang. Scaling up vision-language pre-training for image captioning. *arXiv:2111.12233*, 2021.
- [46] Lun Huang, Wenmin Wang, Jie Chen, and Xiao-Yong Wei. Attention on attention for image captioning. In *International Conference on Computer Vision*, 2019.
- [47] Md Amirul Islam, Matthew Kowal, Sen Jia, Konstantinos G. Derpanis, and Neil D. B. Bruce. Global pooling, more than meets the eye: Position information is encoded channel-wise in CNNs. In *International Conference on Computer Vision*, 2021.
- [48] Andrew Jaegle, Felix Gimeno, Andy Brock, Oriol Vinyals, Andrew Zisserman, and Joao Carreira. Perceiver: General perception with iterative attention. In *International Conference on Machine Learning*, 2021.

- [49] Aashi Jain, Mandy Guo, Krishna Srinivasan, Ting Chen, Sneha Kudugunta, Chao Jia, Yinfei Yang, and Jason Baldridge. MURAL: multimodal, multitask retrieval across languages. *arXiv:2109.05125*, 2021.
- [50] Chao Jia, Yinfei Yang, Ye Xia, Yi-Ting Chen, Zarana Parekh, Hieu Pham, Quoc V. Le, Yun-Hsuan Sung, Zhen Li, and Tom Duerig. Scaling up visual and vision-language representation learning with noisy text supervision. *arXiv:2102.05918*, 2021.
- [51] Alex Jinpeng Wang, Yixiao Ge, Rui Yan, Yuying Ge, Xudong Lin, Guanyu Cai, Jianping Wu, Ying Shan, Xiaohu Qie, and Mike Zheng Shou. All in one: Exploring unified video-language pre-training. *arXiv:2203.07303*, 2022.
- [52] Rafal Jozefowicz, Oriol Vinyals, Mike Schuster, Noam Shazeer, and Yonghui Wu. Exploring the limits of language modeling. *arXiv:1602.02410*, 2016.
- [53] Jared Kaplan, Sam McCandlish, Tom Henighan, Tom B Brown, Benjamin Chess, Rewon Child, Scott Gray, Alec Radford, Jeffrey Wu, and Dario Amodei. Scaling laws for neural language models. *arXiv:2001.08361*, 2020.
- [54] Douwe Kiela, Hamed Firooz, Aravind Mohan, Vedanuj Goswami, Amanpreet Singh, Pratik Ringshia, and Davide Testuggine. The Hateful Memes Challenge: Detecting hate speech in multimodal memes. *Conference on Neural Information Processing Systems*, 2020.
- [55] Hugo Larochelle. Few-shot classification by recycling deep learning. Invited Talk at the *S2D-OLAD Workshop, ICLR 2021*, 2021. URL <https://slideslive.com/38955350/fewshot-classification-by-recycling-deep-learning>.
- [56] Brian Lester, Rami Al-Rfou, and Noah Constant. The power of scale for parameter-efficient prompt tuning. *arXiv:2104.08691*, 2021.
- [57] Junnan Li, Ramprasaath Selvaraju, Akhilesh Gotmare, Shafiq Joty, Caiming Xiong, and Steven Chu Hong Hoi. Align before fuse: Vision and language representation learning with momentum distillation. In *Conference on Neural Information Processing Systems*, 2021.
- [58] Junnan Li, Dongxu Li, Caiming Xiong, and Steven Hoi. BLIP: Bootstrapping language-image pre-training for unified vision-language understanding and generation. *arXiv:2201.12086*, 2022.
- [59] Linjie Li, Yen-Chun Chen, Yu Cheng, Zhe Gan, Licheng Yu, and Jingjing Liu. HERO: Hierarchical encoder for video+language omni-representation pre-training. *arXiv:2005.00200*, 2020.
- [60] Xiang Lisa Li and Percy Liang. Prefix-tuning: Optimizing continuous prompts for generation. *arXiv:2101.00190*, 2021.
- [61] Xiujun Li, Xi Yin, Chunyuan Li, Pengchuan Zhang, Xiaowei Hu, Lei Zhang, Lijuan Wang, Houdong Hu, Li Dong, Furu Wei, Yejin Choi, and Jianfeng Gao. Oscar: Object-semantics aligned pre-training for vision-language tasks. In *European Conference on Computer Vision*, 2020.
- [62] Phillip Lippe, Nithin Holla, Shantanu Chandra, Santhosh Rajamanickam, Georgios Antoniou, Ekaterina Shutova, and Helen Yannakoudakis. A multimodal framework for the detection of hateful memes. *arXiv:2012.12871*, 2020.
- [63] Jiachang Liu, Dinghan Shen, Yizhe Zhang, Bill Dolan, Lawrence Carin, and Weizhu Chen. What makes good in-context examples for GPT-3? *arXiv:2101.06804*, 2021.
- [64] Siqi Liu, Zhenhai Zhu, Ning Ye, Sergio Guadarrama, and Kevin Murphy. Optimization of image description metrics using policy gradient methods. In *International Conference on Computer Vision*, 2017.
- [65] Yu Liu, Lianghua Huang, Liuyihang Song, Bin Wang, Yingya Zhang, and Pan Pan. Enhancing textual cues in multi-modal transformers for VQA. *VizWiz Challenge 2021*, 2021.

- [66] Jiasen Lu, Dhruv Batra, Devi Parikh, and Stefan Lee. ViLBERT: Pretraining task-agnostic visiolinguistic representations for vision-and-language tasks. *Conference on Neural Information Processing Systems*, 2019.
- [67] Huaishao Luo, Lei Ji, Botian Shi, Haoyang Huang, Nan Duan, Tianrui Li, Jason Li, Taroon Bharti, and Ming Zhou. UniVL: A unified video and language pre-training model for multi-modal understanding and generation. *arXiv:2002.06353*, 2020.
- [68] Ziyang Luo, Yadong Xi, Rongsheng Zhang, and Jing Ma. VC-GPT: Visual conditioned GPT for end-to-end generative vision-and-language pre-training. *arXiv:2201.12723*, 2022.
- [69] Kenneth Marino, Mohammad Rastegari, Ali Farhadi, and Roozbeh Mottaghi. OK-VQA: A visual question answering benchmark requiring external knowledge. In *IEEE Computer Vision and Pattern Recognition*, 2019.
- [70] Ellen M. Markman. *Categorization and naming in children: Problems of induction*. MIT Press, 1989.
- [71] Michael McCloskey and Neil J. Cohen. Catastrophic interference in connectionist networks: The sequential learning problem. *The Psychology of Learning and Motivation*, 1989.
- [72] Jacob Menick, Maja Trebacz, Vladimir Mikulik, John Aslanides, Francis Song, Martin Chadwick, Mia Glaese, Susannah Young, Lucy Campbell-Gillingham, Geoffrey Irving, and Nat McAleese. Teaching language models to support answers with verified quotes. *arXiv:2203.11147*, 2022.
- [73] Antoine Miech, Jean-Baptiste Alayrac, Ivan Laptev, Josef Sivic, and Andrew Zisserman. RareAct: A video dataset of unusual interactions. *arxiv:2008.01018*, 2020.
- [74] Antoine Miech, Jean-Baptiste Alayrac, Lucas Smaira, Ivan Laptev, Josef Sivic, and Andrew Zisserman. End-to-end learning of visual representations from uncurated instructional videos. In *IEEE Computer Vision and Pattern Recognition*, 2020.
- [75] Tomas Mikolov, Martin Karafiat, Lukas Burget, Jan Cernocky, and Sanjeev Khudanpur. Recurrent neural network based language model. *Interspeech*, 2010.
- [76] Sewon Min, Xinxi Lyu, Ari Holtzman, Mikel Artetxe, Mike Lewis, Hannaneh Hajishirzi, and Luke Zettlemoyer. Rethinking the role of demonstrations: What makes in-context learning work? *arXiv:2202.12837*, 2022.
- [77] Margaret Mitchell, Simone Wu, Andrew Zaldivar, Parker Barnes, Lucy Vasserman, Ben Hutchinson, Elena Spitzer, Inioluwa Deborah Raji, and Timnit Gebru. Model cards for model reporting. In *ACM Conference on Fairness, Accountability, and Transparency*, 2019.
- [78] Ron Mokady, Amir Hertz, and Amit H. Bermano. ClipCap: CLIP prefix for image captioning. *arXiv:2111.09734*, 2021.
- [79] Vishvak Murahari, Dhruv Batra, Devi Parikh, and Abhishek Das. Large-scale pretraining for visual dialog: A simple state-of-the-art baseline. In *European Conference on Computer Vision*, 2020.
- [80] Ethan Perez, Douwe Kiela, and Kyunghyun Cho. True few-shot learning with language models. *Conference on Neural Information Processing Systems*, 2021.
- [81] Ethan Perez, Saffron Huang, Francis Song, Trevor Cai, Roman Ring, John Aslanides, Amelia Glaese, Nat McAleese, and Geoffrey Irving. Red teaming language models with language models. *arXiv:2202.03286*, 2022.
- [82] Hieu Pham, Zihang Dai, Golnaz Ghiasi, Hanxiao Liu, Adams Wei Yu, Minh-Thang Luong, Mingxing Tan, and Quoc V. Le. Combined scaling for zero-shot transfer learning. *arXiv:2111.10050*, 2021.
- [83] Ofir Press, Noah Smith, and Mike Lewis. Train short, test long: Attention with linear biases enables input length extrapolation. In *International Conference on Learning Representations*, 2022.

- [84] Yixuan Qiao, Hao Chen, Jun Wang, Yihao Chen, Xianbin Ye, Ziliang Li, Xianbiao Qi, Peng Gao, and Guotong Xie. Winner team Mia at TextVQA Challenge 2021: Vision-and-language representation learning with pre-trained sequence-to-sequence model. *arXiv:2106.15332*, 2021.
- [85] Alec Radford, Jong Wook Kim, Chris Hallacy, Aditya Ramesh, Gabriel Goh, Sandhini Agarwal, Girish Sastry, Amanda Askell, Pamela Mishkin, Jack Clark, Gretchen Krueger, and Ilya Sutskever. Learning transferable visual models from natural language supervision. *arXiv:2103.00020*, 2021.
- [86] Jack W. Rae, Sebastian Borgeaud, Trevor Cai, Katie Millican, Jordan Hoffmann, Francis Song, John Aslanides, Sarah Henderson, Roman Ring, Susannah Young, Eliza Rutherford, Tom Hennigan, Jacob Menick, Albin Cassirer, Richard Powell, George van den Driessche, Lisa Anne Hendricks, Maribeth Rauh, Po-Sen Huang, Amelia Glaese, Johannes Welbl, Sumanth Dathathri, Saffron Huang, Jonathan Uesato, John Mellor, Irina Higgins, Antonia Creswell, Nat McAleese, Amy Wu, Erich Elsen, Siddhant Jayakumar, Elena Buchatskaya, David Budden, Esme Sutherland, Karen Simonyan, Michela Paganini, Laurent Sifre, Lena Martens, Xiang Lorraine Li, Adhiguna Kuncoro, Aida Nematzadeh, Elena Gribovskaya, Domenic Donato, Angeliki Lazaridou, Arthur Mensch, Jean-Baptiste Lespiau, Maria Tsimoulkelli, Nikolai Grigorev, Doug Fritz, Thibault Sottiaux, Mantas Pajarskas, Toby Pohlen, Zhitao Gong, Daniel Toyama, Cyprien de Masson d'Autume, Yujia Li, Tayfun Terzi, Vladimir Mikulik, Igor Babuschkin, Aidan Clark, Diego de Las Casas, Aurelia Guy, Chris Jones, James Bradbury, Matthew Johnson, Blake Hechtman, Laura Weidinger, Iason Gabriel, William Isaac, Ed Lockhart, Simon Osindero, Laura Rimell, Chris Dyer, Oriol Vinyals, Kareem Ayoub, Jeff Stanway, Lorrayne Bennett, Demis Hassabis, Koray Kavukcuoglu, and Geoffrey Irving. Scaling language models: Methods, analysis & insights from training Gopher. *arXiv:2112.11446*, 2021.
- [87] Colin Raffel, Noam Shazeer, Adam Roberts, Katherine Lee, Sharan Narang, Michael Matena, Yanqi Zhou, Wei Li, and Peter J. Liu. Exploring the limits of transfer learning with a unified text-to-text transformer. *arXiv:1910.10683*, 2019.
- [88] Samyam Rajbhandari, Jeff Rasley, Olatunji Ruwase, and Yuxiong He. ZeRO: Memory optimizations toward training trillion parameter models. In *International Conference for High Performance Computing, Networking, Storage and Analysis*, 2020.
- [89] Aditya Ramesh, Prafulla Dhariwal, Alex Nichol, Casey Chu, and Mark Chen. Hierarchical text-conditional image generation with clip latents. *arXiv:2204.06125*, 2022.
- [90] Steven J. Rennie, Etienne Marcheret, Youssef Mroueh, Jarret Ross, and Vaibhava Goel. Self-critical sequence training for image captioning. In *IEEE Computer Vision and Pattern Recognition*, 2017.
- [91] James Requeima, Jonathan Gordon, John Bronskill, Sebastian Nowozin, and Richard E. Turner. Fast and flexible multi-task classification using conditional neural adaptive processes. *Conference on Neural Information Processing Systems*, 2019.
- [92] Laria Reynolds and Kyle McDonell. Prompt programming for large language models: Beyond the few-shot paradigm. In *Extended Abstracts of the 2021 CHI Conference on Human Factors in Computing Systems*, 2021.
- [93] Rachel Rudinger, Jason Naradowsky, Brian Leonard, and Benjamin Van Durme. Gender bias in coreference resolution. *arXiv:1804.09301*, 2018.
- [94] Olga Russakovsky, Jia Deng, Hao Su, Jonathan Krause, Sanjeev Satheesh, Sean Ma, Zhiheng Huang, Andrej Karpathy, Aditya Khosla, Michael Bernstein, Alexander C. Berg, and Li Fei-Fei. ImageNet large scale visual recognition challenge. *International Journal of Computer Vision*, 2015.
- [95] Victor Sanh, Albert Webson, Colin Raffel, Stephen H. Bach, Lintang Sutawika, Zaid Alyafeai, Antoine Chaffin, Arnaud Stiegler, Teven Le Scao, Arun Raja, Manan Dey, M. Saiful Bari, Canwen Xu, Urmish Thakker, Shanya Sharma Sharma, Eliza Szczechla, Taewoon Kim, Gunjan

- Chhablani, Nihal Nayak, Debajyoti Datta, Jonathan Chang, Mike Tian-Jian Jiang, Han Wang, Matteo Manica, Sheng Shen, Zheng Xin Yong, Harshit Pandey, Rachel Bawden, Thomas Wang, Trishala Neeraj, Jos Rozen, Abheesht Sharma, Andrea Santilli, Thibault Fevry, Jason Alan Fries, Ryan Teehan, Stella Biderman, Leo Gao, Tali Bers, Thomas Wolf, and Alexander M. Rush. Multitask Prompted Training Enables Zero-Shot Task Generalization. In *International Conference on Learning Representations*, 2022.
- [96] Christoph Schuhmann, Richard Vencu, Romain Beaumont, Robert Kaczmarczyk, Clayton Mullis, Aarush Katta, Theo Coombes, Jenia Jitsev, and Aran Komatsuzaki. Laion-400m: Open dataset of clip-filtered 400 million image-text pairs. *arXiv:2111.02114*, 2021.
 - [97] Carsten Schwemmer, Carly Knight, Emily D. Bello-Pardo, Stan Oklobdzija, Martijn Schoonvelde, and Jeffrey W. Lockhart. Diagnosing gender bias in image recognition systems. *Socius*, 2020.
 - [98] Piyush Sharma, Nan Ding, Sebastian Goodman, and Radu Soricut. Conceptual Captions: A cleaned, hypernymed, image alt-text dataset for automatic image captioning. In *Annual Meeting of the Association for Computational Linguistics*, 2018.
 - [99] Mohammad Shoeybi, Mostafa Patwary, Raul Puri, Patrick LeGresley, Jared Casper, and Bryan Catanzaro. Megatron-LM: Training multi-billion parameter language models using model parallelism. *arXiv:2104.08691*, 2019.
 - [100] Amanpreet Singh, Vivek Natarajan, Meet Shah, Yu Jiang, Xinlei Chen, Dhruv Batra, Devi Parikh, and Marcus Rohrbach. Towards VQA models that can read. In *IEEE Computer Vision and Pattern Recognition*, 2019.
 - [101] Amanpreet Singh, Ronghang Hu, Vedanuj Goswami, Guillaume Couairon, Wojciech Galuba, Marcus Rohrbach, and Douwe Kiela. FLAVA: A foundational language and vision alignment model. *arXiv:2112.04482*, 2021.
 - [102] Lucas Smaira, João Carreira, Eric Noland, Ellen Clancy, Amy Wu, and Andrew Zisserman. A short note on the Kinetics-700-2020 human action dataset. *arXiv:2010.10864*, 2020.
 - [103] Jake Snell, Kevin Swersky, and Richard Zemel. Prototypical networks for few-shot learning. *Conference on Neural Information Processing Systems*, 2017.
 - [104] David R So, Wojciech Mańke, Hanxiao Liu, Zihang Dai, Noam Shazeer, and Quoc V. Le. Primer: Searching for efficient transformers for language modeling. *arXiv:2109.08668*, 2021.
 - [105] Emma Strubell, Ananya Ganesh, and Andrew McCallum. Energy and policy considerations for deep learning in NLP. *arXiv:1906.02243*, 2019.
 - [106] Weijie Su, Xizhou Zhu, Yue Cao, Bin Li, Lewei Lu, Furu Wei, and Jifeng Dai. VL-BERT: Pre-training of generic visual-linguistic representations. *arXiv:1908.08530*, 2019.
 - [107] Chen Sun, Austin Myers, Carl Vondrick, Kevin Murphy, and Cordelia Schmid. VideoBERT: A joint model for video and language representation learning. In *International Conference on Computer Vision*, 2019.
 - [108] Ilya Sutskever, James Martens, and Geoffrey E. Hinton. Generating text with recurrent neural networks. In *International Conference on Machine Learning*, 2011.
 - [109] Hao Tan and Mohit Bansal. LXMERT: Learning cross-modality encoder representations from transformer. In *Conference on Empirical Methods in Natural Language Processing*, 2019.
 - [110] Bart Thomee, David A Shamma, Gerald Friedland, Benjamin Elizalde, Karl Ni, Douglas Poland, Damian Borth, and Li-Jia Li. YFCC100M: The new data in multimedia research. *Communications of the ACM*, 2016.
 - [111] Romal Thoppilan, Daniel De Freitas, Jamie Hall, Noam Shazeer, Apoorv Kulshreshtha, Heng-Tze Cheng, Alicia Jin, Taylor Bos, Leslie Baker, Yu Du, YaGuang Li, Hongrae Lee, Huaixiu Steven Zheng, Amin Ghafouri, Marcelo Menegali, Yanping Huang, Maxim Krikun, Dmitry Lepikhin, James Qin, Dehao Chen, Yuanzhong Xu, Zhifeng Chen, Adam Roberts,

- Maarten Bosma, Vincent Zhao, Yanqi Zhou, Chung-Ching Chang, Igor Krivokon, Will Rusch, Marc Pickett, Pranesh Srinivasan, Laichee Man, Kathleen Meier-Hellstern, Meredith Ringel Morris, Tulsee Doshi, Renelito Delos Santos, Toju Duke, Johnny Soraker, Ben Zevenbergen, Vinodkumar Prabhakaran, Mark Diaz, Ben Hutchinson, Kristen Olson, Alejandra Molina, Erin Hoffman-John, Josh Lee, Lora Aroyo, Ravi Rajakumar, Alena Butryna, Matthew Lamm, Viktoriya Kuzmina, Joe Fenton, Aaron Cohen, Rachel Bernstein, Ray Kurzweil, Blaise Aguera-Arcas, Claire Cui, Marian Croak, Ed Chi, and Quoc Le. LaMDA: Language models for dialog applications. *arXiv:2201.08239*, 2022.
- [112] Yonglong Tian, Yue Wang, Dilip Krishnan, Joshua B. Tenenbaum, and Phillip Isola. Rethinking few-shot image classification: a good embedding is all you need? In *European Conference on Computer Vision*, 2020.
 - [113] Hugo Touvron, Andrea Vedaldi, Matthijs Douze, and Hervé Jégou. Fixing the train-test resolution discrepancy. *Conference on Neural Information Processing Systems*, 2019.
 - [114] Maria Tsimpoukelli, Jacob Menick, Serkan Cabi, SM Eslami, Oriol Vinyals, and Felix Hill. Multimodal few-shot learning with frozen language models. *Conference on Neural Information Processing Systems*, 2021.
 - [115] Ashish Vaswani, Noam Shazeer, Niki Parmar, Jakob Uszkoreit, Llion Jones, Aidan N. Gomez, Łukasz Kaiser, and Illia Polosukhin. Attention is all you need. In *Conference on Neural Information Processing Systems*, 2017.
 - [116] Oriol Vinyals, Alexander Toshev, Samy Bengio, and Dumitru Erhan. Show and tell: A neural image caption generator. In *International Conference on Computer Vision*, 2015.
 - [117] Oriol Vinyals, Charles Blundell, Timothy Lillicrap, Koray Kavukcuoglu, and Daan Wierstra. Matching networks for one shot learning. *Conference on Neural Information Processing Systems*, 2016.
 - [118] Jianfeng Wang, Xiaowei Hu, Zhe Gan, Zhengyuan Yang, Xiyang Dai, Zicheng Liu, Yumao Lu, and Lijuan Wang. UFO: A unified transformer for vision-language representation learning. *arXiv:2111.10023*, 2021.
 - [119] Peng Wang, An Yang, Rui Men, Junyang Lin, Shuai Bai, Zhikang Li, Jianxin Ma, Chang Zhou, Jingren Zhou, and Hongxia Yang. Unifying architectures, tasks, and modalities through a simple sequence-to-sequence learning framework. *arXiv:2202.03052*, 2022.
 - [120] Thomas Wang, Adam Roberts, Daniel Hesslow, Teven Le Scao, Hyung Won Chung, Iz Beltagy, Julien Launay, and Colin Raffel. What language model architecture and pretraining objective work best for zero-shot generalization? *arXiv:2204.05832*, 2022.
 - [121] Wenhui Wang, Hangbo Bao, Li Dong, and Furu Wei. VLMo: Unified vision-language pre-training with mixture-of-modality-experts. *arXiv:2111.02358*, 2021.
 - [122] Xin Wang, Jiawei Wu, Junkun Chen, Lei Li, Yuan-Fang Wang, and William Yang Wang. VATEX: A large-scale, high-quality multilingual dataset for video-and-language research. In *International Conference on Computer Vision*, 2019.
 - [123] Yue Wang, Shafiq Joty, Michael Lyu, Irwin King, Caiming Xiong, and Steven Hoi. VD-BERT: A unified vision and dialog transformer with BERT. In *Conference on Empirical Methods in Natural Language Processing*, 2020.
 - [124] Zirui Wang, Jiahui Yu, Adams Wei Yu, Zihang Dai, Yulia Tsvetkov, and Yuan Cao. SimVLM: Simple visual language model pretraining with weak supervision. *arXiv:2108.10904*, 2021.
 - [125] Jason Wei, Maarten Bosma, Vincent Y. Zhao, Kelvin Guu, Adams Wei Yu, Brian Lester, Nan Du, Andrew M. Dai, and Quoc V. Le. Finetuned language models are zero-shot learners. *arXiv:2109.01652*, 2021.

- [126] Laura Weidinger, John Mellor, Maribeth Rauh, Conor Griffin, Jonathan Uesato, Po-Sen Huang, Myra Cheng, Mia Glaese, Borja Balle, Atoosa Kasirzadeh, Zac Kenton, Sasha Brown, Will Hawkins, Tom Stepleton, Courtney Biles, Abeba Birhane, Julia Haas, Laura Rimell, Lisa Anne Hendricks, William Isaac, Sean Legassick, Geoffrey Irving, and Iason Gabriel. Ethical and social risks of harm from language models. *arXiv:2112.04359*, 2021.
- [127] Mitchell Wortsman, Gabriel Ilharco, Samir Yitzhak Gadre, Rebecca Roelofs, Raphael Gontijo-Lopes, Ari S. Morcos, Hongseok Namkoong, Ali Farhadi, Yair Carmon, Simon Kornblith, and Ludwig Schmidt. Model soups: averaging weights of multiple fine-tuned models improves accuracy without increasing inference time. *arXiv:2203.05482*, 2022.
- [128] Bo Wu, Shoubin Yu, Zhenfang Chen, Joshua B. Tenenbaum, and Chuang Gan. STAR: A Benchmark for Situated Reasoning in Real-World Videos. In *Conference on Neural Information Processing Systems*, 2021.
- [129] Junbin Xiao, Xindi Shang, Angela Yao, and Tat-Seng Chua. Next-QA: Next phase of question-answering to explaining temporal actions. In *IEEE Computer Vision and Pattern Recognition*, 2021.
- [130] Dejing Xu, Zhou Zhao, Jun Xiao, Fei Wu, Hanwang Zhang, Xiangnan He, and Yueting Zhuang. Video question answering via gradually refined attention over appearance and motion. In *ACM Multimedia*, 2017.
- [131] Hanwei Xu, Yujun Chen, Yulun Du, Nan Shao, Yanggang Wang, Haiyu Li, and Zhilin Yang. Zeroprompt: Scaling prompt-based pretraining to 1,000 tasks improves zero-shot generalization. *arXiv:2201.06910*, 2022.
- [132] Hu Xu, Gargi Ghosh, Po-Yao Huang, Prahal Arora, Masoumeh Aminzadeh, Christoph Feichtenhofer, Florian Metze, and Luke Zettlemoyer. VLM: Task-agnostic video-language model pre-training for video understanding. *arXiv:2105.09996*, 2021.
- [133] Ming Yan, Haiyang Xu, Chenliang Li, Junfeng Tian, Bin Bi, Wei Wang, Weihua Chen, Xianzhe Xu, Fan Wang, Zheng Cao, Zhicheng Zhang, Qiyu Zhang, Ji Zhang, Songfang Huang, Fei Huang, Luo Si, and Rong Jin. Achieving human parity on visual question answering. *arXiv:2111.08896*, 2021.
- [134] Shen Yan, Xuehan Xiong, Anurag Arnab, Zhichao Lu, Mi Zhang, Chen Sun, and Cordelia Schmid. Multiview transformers for video recognition. *arXiv:2201.04288*, 2022.
- [135] Antoine Yang, Antoine Miech, Josef Sivic, Ivan Laptev, and Cordelia Schmid. Just ask: Learning to answer questions from millions of narrated videos. In *International Conference on Computer Vision*, 2021.
- [136] Zhengyuan Yang, Zhe Gan, Jianfeng Wang, Xiaowei Hu, Yumao Lu, Zicheng Liu, and Lijuan Wang. An empirical study of GPT-3 for few-shot knowledge-based VQA. In *National Conference on Artificial Intelligence (AAAI)*, 2021.
- [137] Zhengyuan Yang, Yijuan Lu, Jianfeng Wang, Xi Yin, Dinei Florencio, Lijuan Wang, Cha Zhang, Lei Zhang, and Jiebo Luo. TAP: Text-aware pre-training for text-VQA and text-caption. In *IEEE Computer Vision and Pattern Recognition*, 2021.
- [138] Lewei Yao, Runhui Huang, Lu Hou, Guansong Lu, Minzhe Niu, Hang Xu, Xiaodan Liang, Zhenguo Li, Xin Jiang, and Chunjing Xu. FILIP: Fine-grained interactive language-image pre-training. *arXiv:2111.07783*, 2021.
- [139] Peter Young, Alice Lai, Micah Hodosh, and Julia Hockenmaier. From image descriptions to visual denotations: New similarity metrics for semantic inference over event descriptions. *Annual Meeting of the Association for Computational Linguistics*, 2014.
- [140] Lu Yuan, Dongdong Chen, Yi-Ling Chen, Noel Codella, Xiyang Dai, Jianfeng Gao, Houdong Hu, Xuedong Huang, Boxin Li, Chunyuan Li, Ce Liu, Mengchen Liu, Zicheng Liu, Yumao Lu, Yu Shi, Lijuan Wang, Jianfeng Wang, Bin Xiao, Zhen Xiao, Jianwei Yang, Michael Zeng, Luowei Zhou, and Pengchuan Zhang. Florence: A new foundation model for computer vision. *arXiv:2111.11432*, 2021.

- [141] Elad Ben Zaken, Shauli Ravfogel, and Yoav Goldberg. BitFit: Simple parameter-efficient fine-tuning for transformer-based masked language-models. *arXiv:2106.10199*, 2021.
- [142] Rowan Zellers, Ximing Lu, Jack Hessel, Youngjae Yu, Jae Sung Park, Jize Cao, Ali Farhadi, and Yejin Choi. MERLOT: Multimodal neural script knowledge models. *Conference on Neural Information Processing Systems*, 2021.
- [143] Rowan Zellers, Jiasen Lu, Ximing Lu, Youngjae Yu, Yanpeng Zhao, Mohammadreza Salehi, Aditya Kusupati, Jack Hessel, Ali Farhadi, and Yejin Choi. MERLOT reserve: Neural script knowledge through vision and language and sound. In *IEEE Computer Vision and Pattern Recognition*, 2022.
- [144] Andy Zeng, Adrian Wong, Stefan Welker, Krzysztof Choromanski, Federico Tombari, Aveek Purohit, Michael Ryoo, Vikas Sindhwani, Johnny Lee, Vincent Vanhoucke, and Pete Florence. Socratic models: Composing zero-shot multimodal reasoning with language. *arXiv:2204.00598*, 2022.
- [145] Xiaohua Zhai, Alexander Kolesnikov, Neil Houlsby, and Lucas Beyer. Scaling vision transformers. *arXiv:2106.04560*, 2021.
- [146] Xiaohua Zhai, Xiao Wang, Basil Mustafa, Andreas Steiner, Daniel Keysers, Alexander Kolesnikov, and Lucas Beyer. LiT: Zero-shot transfer with locked-image text tuning. *arXiv:2111.07991*, 2021.
- [147] Dora Zhao, Angelina Wang, and Olga Russakovsky. Understanding and evaluating racial biases in image captioning. In *IEEE Computer Vision and Pattern Recognition*, 2021.
- [148] Zihao Zhao, Eric Wallace, Shi Feng, Dan Klein, and Sameer Singh. Calibrate before use: Improving few-shot performance of language models. In *International Conference on Machine Learning*, 2021.
- [149] Luowei Zhou, Chenliang Xu, and Jason J. Corso. Towards automatic learning of procedures from web instructional videos. In *National Conference on Artificial Intelligence (AAAI)*, 2018.
- [150] Luowei Zhou, Hamid Palangi, Lei Zhang, Houdong Hu, Jason Corso, and Jianfeng Gao. Unified vision-language pre-training for image captioning and VQA. In *National Conference on Artificial Intelligence (AAAI)*, 2020.
- [151] Linchao Zhu and Yi Yang. ActBERT: Learning global-local video-text representations. In *IEEE Computer Vision and Pattern Recognition*, 2020.
- [152] Ron Zhu. Enhance multimodal transformer with external label and in-domain pretrain: Hateful meme challenge winning solution. *arXiv:2012.08290*, 2020.
- [153] Xinxin Zhu, Longteng Guo, Peng Yao, Shichen Lu, Wei Liu, and Jing Liu. Vatex video captioning challenge 2020: Multi-view features and hybrid reward strategies for video captioning. *arXiv:1910.11102*, 2019.
- [154] Xizhou Zhu, Jinguo Zhu, Hao Li, Xiaoshi Wu, Xiaogang Wang, Hongsheng Li, Xiaohua Wang, and Jifeng Dai. Uni-Perceiver: Pre-training unified architecture for generic perception for zero-shot and few-shot tasks. *arXiv:2112.01522*, 2021.
- [155] Luisa Zintgraf, Kyriacos Shiarli, Vitaly Kurin, Katja Hofmann, and Shimon Whiteson. Fast context adaptation via meta-learning. In *International Conference on Machine Learning*, 2019.

Checklist

1. For all authors...
 - (a) Do the main claims made in the abstract and introduction accurately reflect the paper's contributions and scope? **[Yes]**
 - (b) Did you describe the limitations of your work? **[Yes]** See Section 5.
 - (c) Did you discuss any potential negative societal impacts of your work? **[Yes]** See Section 5 for a brief discussion and Appendix D.2 for the full discussion.
 - (d) Have you read the ethics review guidelines and ensured that your paper conforms to them? **[Yes]**
2. If you are including theoretical results...
 - (a) Did you state the full set of assumptions of all theoretical results? **[N/A]**
 - (b) Did you include complete proofs of all theoretical results? **[N/A]**
3. If you ran experiments...
 - (a) Did you include the code, data, and instructions needed to reproduce the main experimental results (either in the supplemental material or as a URL)? **[No]** The code and the data are proprietary.
 - (b) Did you specify all the training details (e.g., data splits, hyperparameters, how they were chosen)? **[Yes]** See Section 3 and Appendix B.
 - (c) Did you report error bars (e.g., with respect to the random seed after running experiments multiple times)? **[No]** We do not observe large enough variance in our training runs to justify the computation cost incurred by multiple training runs. For the largest models, it is not feasible within our compute budget.
 - (d) Did you include the total amount of compute and the type of resources used (e.g., type of GPUs, internal cluster, or cloud provider)? **[Yes]** Details can be found in Appendix B.1.2. In short, our largest run was trained on 1536 TPU chips for 15 days.
4. If you are using existing assets (e.g., code, data, models) or curating/releasing new assets...
 - (a) If your work uses existing assets, did you cite the creators? **[Yes]** We properly cited the prior methods on which our work is based, as well as prior datasets when appropriate (e.g., ALIGN).
 - (b) Did you mention the license of the assets? **[N/A]** The assets we used are previous work for which we cited papers. We do mention the license of all visual assets we use for the figures of the paper in Appendix G.
 - (c) Did you include any new assets either in the supplemental material or as a URL? **[No]**
 - (d) Did you discuss whether and how consent was obtained from people whose data you're using/curating? **[Yes]** Our data was automatically scraped from million of webpages. See Datasheets [30] in Appendix F.
 - (e) Did you discuss whether the data you are using/curating contains personally identifiable information or offensive content? **[Yes]** See Datasheets [30] in Appendix F.
5. If you used crowdsourcing or conducted research with human subjects...
 - (a) Did you include the full text of instructions given to participants and screenshots, if applicable? **[N/A]**
 - (b) Did you describe any potential participant risks, with links to Institutional Review Board (IRB) approvals, if applicable? **[N/A]**
 - (c) Did you include the estimated hourly wage paid to participants and the total amount spent on participant compensation? **[N/A]**

Appendix

We provide an overview of the Appendix below.

Method (Appendix A). We first provide additional details about our model in Appendix A.1:

- An illustration and pseudo-code for the Perceiver Resampler (described in Section 2.1) is provided in Appendix A.1.1 and Figure 5.
- A similar illustration is provided for the GATED XATTN-DENSE layer of Section 2.2 in Appendix A.1.2 and Figure 4.
- Details on our implementation of the multi-image/video attention mechanism (Section 2.3) are given in Appendix A.1.3.
- Hyperparameters for all model architectures are given in Appendix A.1.4.

We then explain how we evaluate our models using in-context few-shot learning in Appendix A.2. This includes details on how we build the few-shot prompt, how we get predictions for open- and close-ended tasks, how we obtain the zero-shot numbers, and how we leverage retrieval and ensembling to take advantage of more annotated examples.

Finally, in Appendix A.3, we provide more details on our training datasets:

- Collection of M3W in Appendix A.3.1,
- How we process M3W samples during training in Appendix A.3.2,
- Collection of LTIP and VTP in Appendix A.3.3,
- Deduplication strategy we employ to ensure that there is no leakage between our training and evaluation datasets in Appendix A.3.4.

Experiments (Appendix B). We first provide additional training and evaluation details in Appendix B.1, including:

- Details on *Flamingo*-3B, *Flamingo*-9B and *Flamingo* in Appendix B.1.1,
- The training hyperparameters in Appendix B.1.2,
- More details on the Contrastive model pretraining in Appendix B.1.3,
- Details on our evaluation benchmarks and splits in Appendix B.1.4,
- A discussion on the few-shot learning hyperparameters in Appendix B.1.5,
- The dialogue prompt used in the qualitative dialogue examples shown in Figure 1 and Figure 11 in Appendix B.1.6.

Next, we give additional results obtained by our models in Appendix B.2 including the performance of the Flamingo models on classification tasks in Appendix B.2.1, detailed fine-tuning results in Appendix B.2.2, and zero-shot results from our contrastive models (Appendix B.2.3).

Finally, we provide more ablation studies in Appendix B.3 for both the Flamingo models (Appendix B.3.1) and our contrastive pretrained Visual Encoders (Appendix B.3.2).

Qualitative results (Appendix C). More qualitative results are given in Appendix C: Figure 10 (single image sample), Figure 11 (dialogue examples), and Figure 12 (video examples).

Discussion (Appendix D). We provide a more complete discussion on our work, including limitations, failure cases, broader impacts and societal impacts of our work in Appendix D.

Model card (Appendix E). The *Flamingo* model card is provided in Appendix E.

Datasheets (Appendix F). Datasheets for M3W, LTIP and VTP are respectively given in Appendix F.1, Appendix F.2.1 and Appendix F.2.2.

Credit for visual content (Appendix G). We provide attribution for all visual illustrations used in the paper in Appendix G.

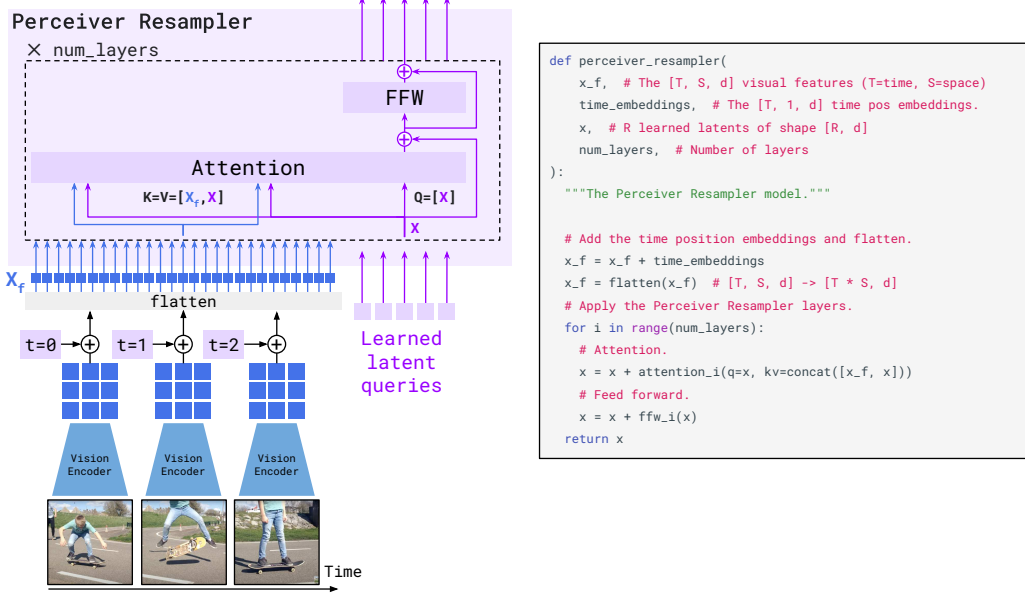


Figure 5: **The Perceiver Resampler** module maps a *variable* size grid of spatio-temporal visual features output by the Vision Encoder to a *fixed* number of output tokens (five in the figure), independently from the input image resolution or the number of input video frames. This transformer has a set of learned latent vectors as queries, and the keys and values are a concatenation of the spatio-temporal visual features with the learned latent vectors.

A Method

A.1 Model details

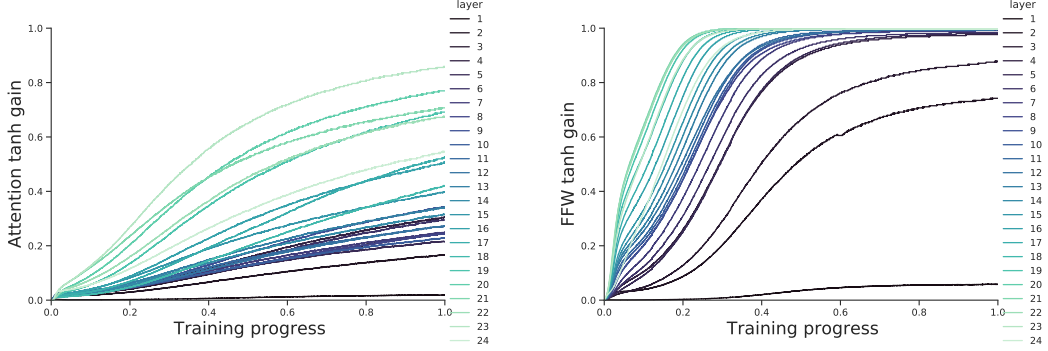
A.1.1 Perceiver Resampler

Expanding on our brief description in Section 2.1, Figure 5 provides an illustration of our Perceiver Resampler processing an example video, together with pseudo-code. Our Perceiver Resampler is similar in spirit to the Perceiver models proposed by Jaegle et al. [48]. We learn a predefined number of latent input queries, and cross-attend to the flattened visual features X_f . These visual features X_f are obtained by first adding a learnt temporal position encoding to each feature within a given video frame (an image being considered as a single-frame video). Note that we only use temporal encodings and no explicit spatial grid position encodings; we did not observe improvements from the latter. This rationale behind is likely that CNNs, such as our NFNet encoder, are known to implicitly include spatial information channel-wise [47]. The visual features are then flattened and concatenated as illustrated in Figure 5. The number of output tokens of the Perceiver Resampler is equal to the number of learnt latent queries. Unlike in DETR and Perceiver, the keys and values computed from the learnt latents are concatenated to the keys and values obtained from X_f , which we found to perform slightly better.

A.1.2 GATED XATTN-DENSE details

We provide in Figure 4 an illustration of a GATED XATTN-DENSE block and how it connects to a frozen LM block, together with pseudo-code.

We also plot in Figure 6 the evolution of the absolute value of the tanh gating values as a function of training progress (from 0% to 100%) at different layers of the LM stack for the *Flamingo-3B* model composed of 24 LM layers. All layers of the frozen LM stack seem to utilize the visual information as the tanh gating absolute values quickly grow in absolute value from their 0 initializations. We also note that the absolute values seem to grow with the depth. However, it is difficult to draw strong conclusions from this observation: the scale of the activations before gating may also vary with depth.



(a) Attention tanh gating

(b) FFW tanh gating.

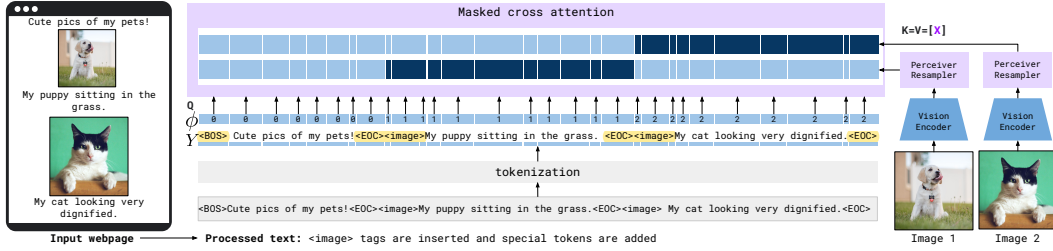
Figure 6: Evolution of the absolute value of the tanh gating at different layers of *Flamingo-3B*.

Figure 7: **Interleaved visual data and text support.** Given text interleaved with images/videos, e.g. coming from a webpage, we first process the text by inserting `<image>` tags at the locations of the visual data in the text as well as special tokens (`<BOS>` for “beginning of sequence” or `<EOC>` for “end of chunk”). Images are processed independently by the Vision Encoder and Perceiver Resampler to extract visual tokens. At a given text token, the model only cross-attends to the visual tokens corresponding to the last preceding image/video. ϕ indicates which image/video a text token can attend or 0 when no image/video is preceding. In practice, this selective cross-attention is achieved through masking – illustrated here with the dark blue entries (unmasked/visible) and light blue entries (masked).

Future work is required to better understand the effect of these added layers on the optimization dynamics and on the model itself.

A.1.3 Multi-visual input support

We illustrate in Figure 7 the masking approach we use to limit the number of visual tokens that a certain text token sees. We also formalize our notation for the interleaved sequences of images/videos and text.

Interleaved sequences of visual data and text. We consider interleaved image/video and text examples: each example holds a sequence of text y , a sequence of images/videos x , and the sequence of positions of the images in the text. Based on the visual data positions, we define a function $\phi : [1, L] \mapsto [0, N]$ that assigns to each text position the index of the last image/video appearing before this position (or 0 if no visual data appears before the position). The function ϕ defines which visual inputs we consider usable to predict token ℓ in Equation (1): the set of preceding tokens $y_{<\ell} \triangleq (y_1, \dots, y_{\ell-1})$, and the set of preceding images/videos $x_{\leq \ell} \triangleq \{x_i | i \leq \phi(\ell)\}$.

A.1.4 Transformer architecture

We list in Table 4 the number of layers (L), the hidden dimension (D), the number of heads (H), and the FFW activation (Act.) used for each transformer component of our Flamingo models. The dimension of keys and values in each configuration is given by D/H (96 for the Perceiver Resampler; 128 for GATED XATTN-DENSE and the frozen LM), and the hidden dimension of each feed-forward

	Perceiver Resampler				GATED XATTN-DENSE				Frozen LM			
	L	D	H	Act.	L	D	H	Act.	L	D	H	Act.
Flamingo-3B	6	1536	16	Sq. ReLU	24	2048	16	Sq. ReLU	24	2048	16	GeLU
Flamingo-9B	6	1536	16	Sq. ReLU	10	4096	32	Sq. ReLU	40	4096	32	GeLU
Flamingo	6	1536	16	Sq. ReLU	12	8192	64	Sq. ReLU	80	8192	64	GeLU

Table 4: Hyper-parameters for the Flamingo models’ transformers. The hidden size of each feed-forward MLP is $4D$. **L**: number of layers, **D**: transformer hidden size, **H**: number of heads, **Act.**: FFW activation, **Sq. ReLU**: Squared ReLU [104].

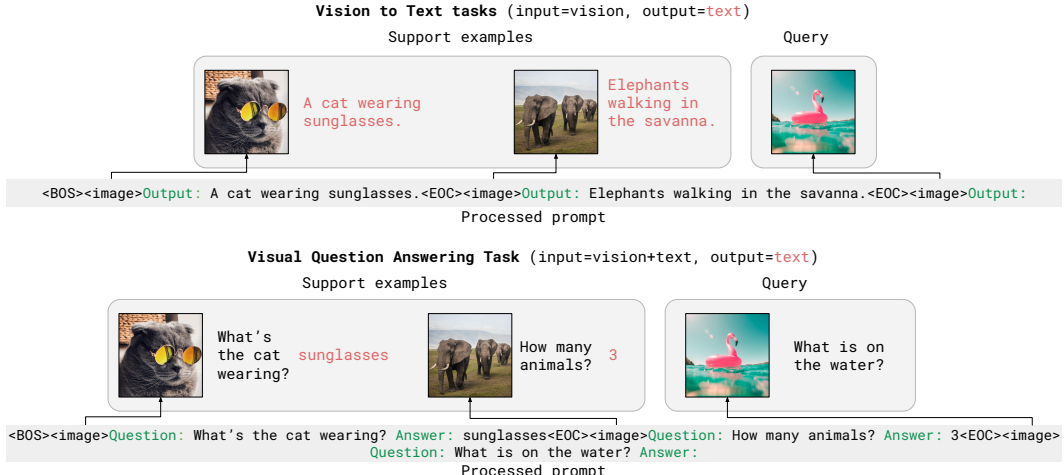


Figure 8: **Few-shot interleaved prompt generation.** Given some task-specific few-shot examples (a.k.a. support examples) and a query for which Flamingo should make a prediction, we build the prompt by interleaving images with their corresponding texts. We introduce some formatting to do this, prepending “**Output:**” to the expected response for all vision-to-text tasks or prompting in the format “**Question:** {question} **Answer:** {answer}” for visual question-answering tasks.

MLP is $4D$. Note that the frozen LM was trained with the GeLU activation [39], while the remaining trainable transformer layers use the Squared ReLU activation [104], which we found to outperform GeLU.

A.2 In-context few-shot evaluation details

In-context learning with Flamingo models. We evaluate the ability of our models to rapidly adapt to new tasks using in-context learning, following an analogous approach to the one used in GPT-3 [11]. In detail, we are given a set of support examples in the form of $(image, text)$ or $(video, text)$ (where the *image* or *video* is the input visual and the *text* is the expected response and any additional task-specific information, e.g., a question) and a single visual query for which we want our model to make a prediction. Given this, we build a multimodal prompt by concatenating the support examples followed by the visual query as illustrated by Figure 8. Unless specified otherwise, we choose the concatenation order at random.

Open-ended and close-ended evaluations. In an open-ended setting, the model’s sampled text following the query image is then taken as its prediction for the image, stopping at the first `<EOC>` (“end of chunk”) token prediction. Unless specified otherwise, we always use beam search with a beam size of 3. In a close-ended setting, all possible outputs are independently appended to the query image, and we score each of the resulting sequences using the log-likelihood estimated by our model. These scores are then used to rank the candidate outputs in decreasing order, from most confident to least confident.



Figure 9: **Training datasets.** Mixture of training datasets of different formats. N corresponds to the number of visual inputs for a single example. For paired image (or video) and text datasets, $N = 1$. T is the number of video frames ($T = 1$ for images). H , W , and C are height, width and color channels.

Zero-shot generalization. In the absence of few-shot examples, approaches commonly rely on prompt engineering [85] to condition the model at inference using a suitable natural language description of the task. Validation of such prompts can significantly impact performance but requires access to a number of annotated examples and cannot therefore be considered truly zero-shot. Furthermore, Perez et al. [80] have shown that such validation procedures are generally not robust with access to only a handful of samples during validation. To report zero-shot performance in our work, we instead build a prompt with *two examples* from the downstream tasks *where we remove their corresponding images or videos*. For example, for the task illustrated at the top of Figure 8, the prompt would be “<BOS>Output: This is a cat wearing sunglasses.<EOC>Output: Three elephants walking in the savanna.<EOC><image> Output:” and no support images would be fed to the model. We observed that only showing one, instead of two, text examples in the prompt is highly detrimental as the model is biased towards producing text output similar to the single provided text example. Providing more than two text examples helps but only marginally. We hence use two text examples in all zero-shot results for practicality. In practice, we believe this is not more cumbersome than finding a good natural text description for a given task. This relates to recent findings on the aspects of demonstrations that are key drivers of performance [76]. For close-ended tasks, where we use the model to score different possible answers, we observe it is not necessary to provide a single text example in the zero-shot prompt.

Retrieval-based In-Context Example Selection [136]. When the size of the support set exceeds a certain limit, it can become difficult to leverage all the examples with in-context learning: first because it becomes excessively expensive to fit all the examples in the prompt, and second because there is a risk of poor generalization when the prompt size exceeds the size of the sequence used during training [83]. In such situations, it is appealing to use a form of prompt selection to both limit the sequence length as well as potentially improve the prompt quality which can in turn lead to better performance [63]. In particular, we follow the Retrieval-based In-Context Example Selection (RICES) approach introduced by [136]. In detail, given a query image, we retrieve similar images in the support set by comparing the visual features extracted from our frozen pretrained visual encoder. We then build the prompt by concatenating the top- N most similar examples. Since LMs are sensitive to the ordering in the prompt due to recency bias [148], we order the examples by increasing order of similarity, such that the most similar support example appears right before the query. We notably show the effectiveness of this approach in classification settings with multiple hundreds of classes (see Appendix B.2.1) where we are given one or more images/videos per class, yielding a number of examples that would not otherwise fit in the prompt.

Prompt ensembling. We also explore ensembling the outputs of the model across multiple prompts in the close-ended setting. This can notably be combined with RICES where ensembling can be done over multiple permutations of the ranked nearest neighbors. Specifically, for a given answer, we average the log likelihoods estimated by the model over 6 random permutations of the selected few-shot examples.

A.3 Training dataset details

We train the Flamingo models on a carefully chosen mixture of datasets illustrated in Figure 9 and described next.

A.3.1 M3W collection

The selection and scraping of web pages for *M3W* follows a similar process to the one used for collecting the *MassiveWeb* dataset [86]. We start by filtering out non-English documents. We also remove those that do not pass internal filters, which identify explicit content across images, videos, and text. We use a custom scraper to extract salient content from the remaining documents, in the form of plain text interleaved with images, as described in Section 2.4. The text in *M3W* is collected in a similar fashion to that of *MassiveWeb*, but we also collect any images present at the same level in the HTML tree. We discard documents for which the scraping process does not yield any images.

We then apply similar text filtering heuristics, to remove low quality documents and reduce repetition, as well as some image filters to remove images that are too small (either width or height less than 64 pixels), too wide or narrow (aspect ratio greater than 3 in either direction), or unambiguously low quality (e.g. single-colour images). We discard documents that no longer contain any images following this filtering step.

A.3.2 M3W image-placement augmentation

During evaluation of Flamingo models, we prompt the model with an image and ask it to generate text for that image. This lends itself to a natural sequencing at inference time in which the image comes before the corresponding text output.

However, the correspondence between images and text in our interleaved M3W dataset (Section 2.4) is in general unknown (and potentially not well-defined in certain cases). As a motivating example, a simple webpage might be structured in either of the following ways:

- (a) This is my dog! <dog image> This is my cat! <cat image>
- (b) <dog image> That was my dog! <cat image> That was my cat!

The text-aligned image indices (`indices`) might “ideally” be chosen such that at each point in the text, the index points to the most semantically relevant image for that text – i.e., the next image in example (a), and the previous image in example (b). In the absence of a general way to determine semantic correspondence between text and images on webpages “in the wild”, we make a simplifying assumption that the most relevant image at any given point in the text is either the last image appearing before the text token, or the image immediately following it (as in the simple examples above), and choose `indices` accordingly.

During training, for each webpage sampled, we sample with probability $p_{next} = \frac{1}{2}$ whether `indices` are chosen to map text to the previous or next image. This inevitably means we make the semantically “unnatural” choice – e.g., associating the text “This is my cat!” with the dog image in (a) above – around half of the time. We ablate this choice in Section 3.3, finding a small advantage to setting $p_{next} = \frac{1}{2}$ over either 0 (always the previous image index) or 1 (always the next image index). This suggests that there may be a beneficial “data augmentation” effect to this randomisation.

A.3.3 LTIP and VTP: Visual data paired with text

Along with our interleaved image and text dataset, we use several paired vision and text web datasets for training. One dataset is ALIGN [50], composed of 1.8 billion images paired with alt-text. ALIGN is large, but noisy and limited to images. The images are often poorly described by the corresponding alt-text annotation. For this reason, we augment it with two datasets: LTIP (Long Text & Image Pairs) consists of 312 million images, and VTP (Video & Text Pairs) consists of 27 million short videos (approximately 22 seconds on average). Both datasets are paired with more descriptive captions. For instance, the average number of tokens of an ALIGN text description is 12.4 per image, while it is 20.5 for the LTIP dataset. The LTIP and VTP datasets were collected by crawling fewer than ten websites targeting high-quality and rich image descriptions. These single-image and single-video datasets are preprocessed analogously to the *M3W* data preprocessing described previously, adding the `<image>` tag at the beginning of the sequence (immediately after `<BOS>`), and the `<EOC>` token after the text (before `<EOS>`). We deduplicated these datasets against all our benchmarks (against both the training and the evaluation sets) using image similarity, as detailed in Appendix A.3.4. Datasheets for LTIP and VTP are respectively given in Appendix F.2.1 and Appendix F.2.2.

	Requires model sharding	Frozen Language	Frozen Vision	Trainable GATED XATTN-DENSE	Trainable Resampler	Total count
<i>Flamingo</i> -3B	\times	1.4B	435M	1.2B (every)	194M	3.2B
<i>Flamingo</i> -9B	\times	7.1B	435M	1.6B (every 4th)	194M	9.3B
<i>Flamingo</i>	\checkmark	70B	435M	10B (every 7th)	194M	80B

Table 5: **Parameter counts for Flamingo models.** We focus on increasing the parameter count of the frozen LM and the trainable vision-text GATED XATTN-DENSE modules while maintaining the frozen vision encoder and trainable Resampler to a fixed and small size across the different models. The frequency of the GATED XATTN-DENSE with respect to the original language model blocks is given in parentheses.

A.3.4 Dataset deduplication against evaluation tasks

We used an internal deduplication tool to deduplicate our training datasets from our evaluation datasets. This deduplication pipeline relies on a trained visual encoder which maps embedding closer together when they are potential duplicates. Once the image embeddings have been computed, a fast approximate nearest neighbor search is performed on the training images to retrieve duplicate candidates from the validation datasets. For the paired image-text dataset, we have deduplicated our LTIP and ALIGN training images against: ImageNet (train, val), COCO (train, valid, test), OK-VQA (train, valid, test), VQAv2 (train, valid, test), Flickr30k (train, valid, test), VisDial (train, valid, test).

We did not deduplicate our image datasets against VizWiz, HatefulMemes and TextVQA as we performed these evaluations only after having trained our Flamingo models. However, we believe this had no impact on our results as the images from these datasets are unlikely to be scraped from the web; VizWiz images were obtained using a specific mobile app and only available for download, HatefulMemes memes were created by researchers instead of being scraped on the web and finally TextVQA images are from OpenImages.

Note that we did not run the deduplication on the *M3W* dataset as one training example is a full webpage of interleaved paragraph with several images, unlikely to contain images from our benchmark suite. To verify this hypothesis, we have obtained near-duplicate statistics on the 185M individual images from *M3W* and the results are the following: in total, 1314 potential duplicates were found from the validation and test splits of ImageNet, COCO, OK-VQA, VQAv2, Flickr30k and VisDial. Out of the 1314 candidates, only 125 are exact duplicates.

For the video datasets, we did not perform any deduplication of VTP (27M videos) as none of the collected VTP videos were obtained from YouTube or Flickr, which are the sources of all of our video evaluation datasets collected on the Internet.

B Experiments

B.1 Training and evaluation details

B.1.1 Models

We perform experiments across three model sizes, where we scale the frozen language model from 1.4B to 7B and 70B; and adapt the parameter count of other components accordingly. We keep the pretrained vision encoder frozen across all experiments and use a NFNet-F6 model trained contrastively (see Appendix B.1.3), unless explicitly stated otherwise in the ablation study. We use a Perceiver Resampler with approximately 200M parameters across all three model sizes.

The decision on how many GATED XATTN-DENSE layers to interleave is mainly driven by a trade-off between memory constraints and downstream performance. We identified the optimal trade-off at small model scales, before transferring our findings to the large model architecture.

We obtain three models, *Flamingo*-3B, *Flamingo*-9B and *Flamingo*-80B, detailed below:

- The *Flamingo*-3B model builds on top of a **1.4B frozen language model** from [42]. Before each transformer block, we add a GATED XATTN-DENSE layer attending to the visual inputs; this accounts for 1.4B additional learned parameters.
- The *Flamingo*-9B model builds on top of a **7B frozen language model** from [42]. Starting from the very first layer and before every fourth transformer blocks, we add a GATED XATTN-DENSE layer attending to the visual inputs; this accounts for 1.8B additional learned parameters.
- The *Flamingo*-80B model builds on top of **the frozen Chinchilla 70B** language model [42]. Starting from the very first layer and before every seventh transformer blocks, we add a GATED XATTN-DENSE layer attending to the visual inputs; this accounts for 10B additional learned parameters. For simplicity, we refer to this model as simply *Flamingo* throughout the paper.

In Table 5 we report the parameter count of each component of our models, as well as model sharding requirements. We provide more Transformer architecture details in Appendix A.1.4. The *Flamingo* model card [77] is also given in Appendix E.

B.1.2 Training details for the Flamingo models

Data augmentation and preprocessing. Empirically we find that it is effective to stochastically prepend the paired dataset text samples with a single space character, with probability 0.5. We attribute this to the fact that our subword tokenizer maps the beginning of various words to a different token depending on whether it is preceded by a space. This allows us to enforce invariance to this tokenizer artifact, without degrading significantly correctness of the punctuation which is already lacking in many of these samples. We observe that this leads to substantial improvement across tasks.

The visual inputs are resized to 320×320 while preserving their aspect ratios, padding the image with the mean value if required. Note that this is higher than the 288×288 resolution used for the contrastive pretraining of our Vision Encoder (see Appendix B.1.3). The increase in resolution during the final stage training was motivated by [113] showing one can obtain improved performance at a higher test-time resolution when using CNNs. This increase in resolution also comes with only a moderate computational and memory cost as no backpropagation is performed through the frozen Vision Encoder. We also employ random left/right flips and color augmentation.

For interleaved datasets (Section 2.4) we also employ augmentation by lightly randomizing the selected image indices ϕ with a hyperparameter p_{next} when sampling examples from the *M3W* dataset. This augmentation is detailed in Appendix A.3.2 and our choice of $p_{next} = \frac{1}{2}$ is ablated in Appendix B.3.1. For video training, we temporally sample a clip of 8 frames sampled at one frame per second (fps) from each training video. Although our model was trained with a fixed number of 8 frames, at inference time, we input 30 frames at 3 FPS. This is achieved by linearly interpolating the learnt temporal position embedding of the Perceiver Resampler at inference time.

Loss and optimisation. All our models are trained using the AdamW optimizer with global norm clipping of 1, no weight decay for the Perceiver Resampler and weight decay of 0.1 for the other trainable parameters. The learning rate is increased linearly from 0 to 10^{-4} up over the first 5000 steps then held constant for the duration of training (no improvements were observed from decaying the learning rate). Unless specified otherwise we train our models for 500k steps. Four datasets are used for training: *M3W*, ALIGN, LTIP and VTP with weights λ_m of 1.0, 0.2, 0.2 and 0.03 respectively. These weights were obtained empirically at a small model scale and kept fixed afterwards. Batch sizes depend on the setting and are given in the next sections.

Infrastructure and implementation. Our model and associated infrastructure were implemented using JAX [8] and Haiku [40]. All training and evaluation was performed on TPUv4 instances. The largest model containing 80 billion parameters is trained on 1536 chips for 15 days and sharded across 16 devices. Megatron type sharding [99] is used to enable 16-way model parallelism for all Embedding / Self-Attention / Cross-Attention / FFW layers, while the NFNet vision layers were unsharded. ZeRO stage 1 [88] is used to shard the optimizer state. All trained parameters and optimizer accumulators are stored and updated in float32; all activations and gradients are computed in bfloat16 after downcasting of parameters from float32 to bfloat16. Frozen parameters are stored and applied in bfloat16.

B.1.3 Contrastive model details

The vision encoder is trained from scratch, together with a language encoder. Using these encoders, images and text pairs are separately encoded and projected to a shared embedding space and L2 normalized. From these embeddings, we maximize the similarity of paired embeddings and minimize the similarity of unpaired embeddings, using a multi-class cross-entropy loss, where the paired image-texts are treated as positive examples and the rest of the batch as negative examples. We use the same loss as in CLIP [85], which consists of two contrastive losses, one from text to image and the other from image to text. We use a learnable temperature parameter in the final log-softmax layer [9]. The text-to-image loss is as follows:

$$L_{\text{contrastive:txt2im}} = -\frac{1}{N} \sum_i^N \log \left(\frac{\exp(L_i^\top V_i \beta)}{\sum_j^N \exp(L_i^\top V_j \beta)} \right) \quad (3)$$

And the image-to-text loss is defined analogously:

$$L_{\text{contrastive:im2txt}} = -\frac{1}{N} \sum_i^N \log \left(\frac{\exp(V_i^\top L_i \beta)}{\sum_j^N \exp(V_i^\top L_j \beta)} \right) \quad (4)$$

The sum of the two losses is minimized. Here, V_i and L_i are, respectively, the normalized embedding of the vision and language component of the i -th element of a batch. β is a trainable inverse temperature parameter and N is the number of elements in the batch. We use the BERT [23] architecture for the language encoder. The outputs of the language and vision encoders are mean-pooled (across tokens and spatial locations, respectively) before being projected to the shared embedding space. We only use the weights from the contrastive vision encoder in the main Flamingo models.

The vision encoder is pretrained on the ALIGN and LTIP datasets. The training image resolution is 288×288 , the joint embedding space is size 1376 and the batch size is 16,384. It is trained for 1.2 million parameter update steps, each of which consist of two gradient calculation steps (more details below) on 512 TPUs v4 chips. The learning rate is decayed linearly from 10^{-3} to zero over the course of training. Images have random color augmentation and horizontal flips applied during training. We use the tokenizer employed by Jia et al. [50]. The Adam optimizer is used to optimize the network, and we apply label smoothing of 0.1. We apply 10^{-2} adaptive gradient clipping (AGC) [10] to the NFNet encoder and global norm gradient clipping of 10 for the BERT encoder.

To evaluate the pretrained model, we track zero-shot image classification and retrieval. For zero-shot image classification, we use image-text retrieval between the images and the class names. Following Radford et al. [85] we use “prompt-ensembling” in which we embed multiple texts using templates such as “A photo of a {class_name}” and average the resulting embedding.

B.1.4 Evaluation benchmarks

Our goal is to develop models that can rapidly adapt to diverse and challenging tasks in the few-shot setting. For this, we consider a wide array of popular image and video benchmarks summarized in Table 6. In total we chose 16 multimodal image/video and language benchmarks, spanning tasks that require some language understanding (visual question answering, captioning, visual dialogue) as well as two standard image and video classification benchmarks (ImageNet and Kinetics). Note that for the video datasets collected from YouTube (i.e., all video datasets except NextQA and STAR), we evaluated our model on all the publicly available video as of April 2022.

DEV benchmarks. In order to validate design decisions of our model over the course of the project, we selected five benchmarks from the 16 multimodal image/video and language benchmarks as well as ImageNet and Kinetics for classification as our development set (referred as **DEV**). To maximise its relevance, we choose the most challenging and widely studied benchmarks for captioning, visual question-answering and classification tasks on both images and videos.

Dataset splits for the DEV benchmarks. Concretely, estimating few-shot learning performance of a model consists of adapting it on a set of *support* samples and evaluating it on a set of *query* samples. As a result, any evaluation set should be composed of two disjoint subsets containing respectively the support and the query samples. For the **DEV** benchmarks that are used both to validate design decisions and hyperparameters, as well as to report final performance, we therefore use four subsets:

	Dataset	DEV	Gen.	Custom prompt	Task description	Eval set	Metric
Image	ImageNet-1k [94]	✓			Object classification	Val	Top-1 acc.
	MS-COCO [15]	✓	✓		Scene description	Test	CIDEr
	VQAv2 [3]	✓	✓		Scene understanding QA	Test-dev	VQA acc. [3]
	OKVQA [69]	✓	✓		External knowledge QA	Val	VQA acc. [3]
	Flickr30k [139]		✓		Scene description	Test (Karpathy)	CIDEr
	VizWiz [35]		✓		Scene understanding QA	Test-dev	VQA acc. [3]
	TextVQA [100]		✓		Text reading QA	Val	VQA acc. [3]
	VisDial [20]				Visual Dialogue	Val	NDCG
Video	HatefulMemes [54]			✓	Meme classification	Seen Test	ROC AUC
	Kinetics700 2020 [102]	✓			Action classification	Val	Top-1/5 avg
	VATEX [122]	✓	✓		Event description	Test	CIDEr
	MSVDQA [130]	✓	✓		Event understanding QA	Test	Top-1 acc.
	YouCook2 [149]		✓		Event description	Val	CIDEr
	MSRVTQA [130]	✓			Event understanding QA	Test	Top-1 acc.
	iVQA [135]		✓		Event understanding QA	Test	iVQA acc. [135]
	RareAct [73]			✓	Composite action retrieval	Test	mWAP
	NextQA [129]		✓		Temporal/Causal QA	Test	WUPS
	STAR [128]				Multiple-choice QA	Test	Top-1 acc.

Table 6: **Summary of the evaluation benchmarks.** DEV benchmarks were used to validate general design decision of the Flamingo models. Gen. stands for generative task where we sample text from the VLM. If a task is non-generative it means that we use the VLM to score answers among a given finite set. For most of our tasks we use a common default prompt, hence minimizing task-specific tuning (see Appendix B.1.5).

- *validation support*: contains support samples for validation;
- *validation query*: contains query samples for validation;
- *test support*: contains support samples for final performance estimation;
- *test query*: contains query samples for final performance estimation.

In practice, for the *test query* subset, we use the subset that prior works report results on, for apples-to-apples comparison. While the validation set would be a natural choice for the *validation query* subset, we note that this is not possible for all benchmarks, since some benchmarks do not have an official validation set (e.g. OKVQA) and for others, the validation is commonly used to report final performance in place of the test set (e.g. ImageNet or COCO). For simplicity, we use a subset of the original training set as the *validation query* subset. Finally, we also use additional disjoint subsets of the training set as respectively the *validation support* subset and the *test support* subset.

We now describe in more detail how we form the latter three subsets. For captioning tasks, open-ended evaluation is efficient so we evaluate on a large number of samples. Specifically, for COCO, we use the same number of samples as used in the Karpathy splits for evaluation sets (5000). For VATEX, because the training set is of limited size, we only evaluate over 1024 samples, reserving the rest for support sets. For question-answering tasks, we evaluate over 1024 samples; chosen to make both open- and close-ended evaluation reasonably fast. For image classification tasks, we evaluate over 10 images per class: 10,000 samples for ImageNet, and 7000 samples for Kinetics700. As for the support sets, for both validation and final performance estimation, we use 2048 samples across all tasks, except for classification tasks where we scale this to 32 samples per class, to better estimate expected performance for each class.

Unbiased few-shot performance estimation. Few-shot learning performance estimates on the DEV benchmarks may be biased, in the sense that over the course of this project, design decisions were made based on the performance obtained on these benchmarks. We note that this is the case for prior work which also make use of these benchmarks to validate and ablate their own design decisions. To account for this bias and provide unbiased few-shot learning performance estimates, we report performance on a remaining set of 11 benchmarks. Among those, some span the same open-ended image and video tasks as our DEV benchmarks (captioning and visual question-answering). But we also look at more specific benchmarks in order to explore less explored capabilities. These notably include: TextVQA [100] which specifically assesses OCR capabilities through question-answering;

VisDial [20], a visual dialogue benchmark; HatefulMemes [54] a vision and text classification benchmark; NextQA [129] which specially focuses on causality and temporal relation; STAR [128], a multiple-choice question answering task; and RareAct [73], a benchmark measuring compositionality in action recognition. We emphasize that *we do not validate any design decisions* on these benchmarks and use them solely to estimate unbiased few-shot learning performance after Flamingo training is done.

B.1.5 Few-shot learning evaluation hyperparameters

In few-shot learning, hyperparameter selection implicitly increases the number of shots as it requires additional validation examples. If those are not taken into account, as is often the case in practice, few-shot performance can be overestimated [80]. Similarly, cross-validation of benchmark-specific hyperparameters such as the prompt should be considered as a particularly basic few-shot learning method, where one selects the task-specific prompt over the set of shots. But other learning approaches might be more effective in making use of these labelled examples. Given the negative results reported by [80] in terms of the robustness of cross-validation and unless mentioned otherwise, all benchmarks are run using a single set of evaluation hyperparameters, including the prompts. We optimize hyperparameters jointly across the *validation* subsets of the DEV benchmarks and do not perform any benchmark-specific cross-validation of hyperparameters, aside from a few exceptions, as we detail next.

Except for HatefulMemes and RareAct, we always use the prompt “`Output: {output}`” for all non-question-answering tasks, and “`Question: {question} Answer: {answer}`” for all question-answering / visual dialogue tasks. In particular, for VisDial [20], we use the previously described prompt to encode each questions/answers in the dialogue and the provided image caption is prepended to the dialogue history without any prompt. For HatefulMemes [54], we use a specific prompt to incorporate the OCR information provided as input which is: “`is an image with written: "{meme_text}" on it. Is it hateful? Answer: {answer}`”, where the answer is either yes or no. Note that this is the only dataset where we explicitly provide OCR text “`meme_text`” as input to Flamingo models. For TextVQA, we do not make use of the provided OCR transcripts and instead directly rely on the off-the-shelf OCR capabilities of the Flamingo models. For RareAct, a zero-shot benchmark, we change the verb names to the third person, add an article before each noun and use the prompt “`Caption: a person {verb + object}`”.

B.1.6 Dialogue prompt

For the dialogue examples in Figures 1 and 11, the following prompt is used:

This is a conversation between a human, User, and an intelligent visual AI, Flamingo. User sends images, and Flamingo describes them.

User: <a cat image>

Flamingo: That is a cat. It's a tiny kitten with really cute big ears.

User: <a dinner image>

Flamingo: This is a picture of a group of people having dinner. They are having a great time!

User: Can you guess what are they celebrating?

Flamingo: They might be celebrating the end of a successful project or maybe a birthday?

User: <a graph image>

Flamingo: This is a graph, it looks like a cumulative density function graph.

Model	Method	Prompt size	shots/class	ImageNet top 1	Kinetics700 avg top1/5
SotA	Fine-tuned	-	full	90.9 [127]	89.0 [134]
SotA	Contrastive	-	0	85.7 [82]	69.6 [85]
NFNetF6	Our contrastive	-	0	77.9	62.9
<i>Flamingo</i> -3B	RICES	8	1	70.9	55.9
		16	1	71.0	56.9
		16	5	72.7	58.3
<i>Flamingo</i> -9B	RICES	8	1	71.2	58.0
		16	1	71.7	59.4
		16	5	75.2	60.9
<i>Flamingo</i> -80B	Random	16	≤ 0.02	66.4	51.2
		8	1	71.9	60.4
		16	1	71.7	62.7
	RICES+ensembling	16	5	76.0	63.5

Table 7: **Few-shot results on classification tasks.** The Flamingo models can also be used for standard classification tasks. In particular, we explore having access to support sets bigger than what our current prompt can accommodate (using up to 5000 support examples). In that regime, large gains are obtained by using the RICES method [136] as well as prompt ensembling. We also observe the same trend as with the vision-language benchmarks: bigger models do better and more shots help.

B.2 Additional performance results

B.2.1 Few-shot learning on classification tasks

We consider applying the Flamingo models to well-studied classification benchmarks like ImageNet or Kinetics700. Results are given in Table 7. We observe a similar pattern as in other experiments: larger model tend to perform better. Second, given that few-shot classification tasks often come with more training examples (e.g., 1000 for ImageNet with 1 example per class), using methods to scale to larger support sets is beneficial. RICES (Retrieval In-Context Example Selection [136] described in Appendix A.2) performs substantially better than simply selecting examples randomly for inclusion in the prompt. Indeed, *Flamingo* achieves a 9.2% improvement in ImageNet classification when selecting 16 support examples out of 5000 using RICES, compared to choosing the same number of examples randomly. Ensembling multiple prompts further boosts results. However, note that Flamingo models underperform the current dominant contrastive paradigm for classification tasks; in particular, they underperform the very contrastive model used as their vision encoder (see Appendix D.1 on Flamingo’s limitations for more details). Finally, state-of-the-art zero-shot models on ImageNet such as BASIC [82] and LiT [146] are particularly optimized on classification tasks as they are trained on JFT-3B [145], a dataset with images and labels. Improving the performance of VLMs such as Flamingo on classification tasks is an interesting direction for future work.

B.2.2 Fine-tuning *Flamingo* as a pretrained vision-language model

To fine-tune Flamingo models on a downstream task, we train them on data batches from the task of interest in the same format as the single-image/video datasets described in Section 2.4.

Freezing and hyperparameters. When fine-tuning *Flamingo*, we keep the underlying LM layers frozen and train the same Flamingo layers as during pretraining. We also increase the resolution of the input images from 320×320 to 480×480 . Unlike in the pretraining phase, we also fine-tune the base visual encoder, finding that this typically improves results, likely due in part to the higher input resolution.

We choose certain hyperparameters on a per-task basis by grid search on a validation subset of the training set (or on the official or standard validation set where available). These hyperparameters include the learning rate (ranging from 3×10^{-8} to 1×10^{-5}) and decay schedule (exponential decay

by factors of $10\times$), number of training steps, batch size (either 8 or 16), and whether visual data augmentation (color augmentation, random horizontal flips) is used.

Results. In Table 8, we present additional results for per-task *Flamingo* fine-tuning. When provided access to a large-scale task-specific dataset with many thousands of examples, we find that we can improve results over our previously presented in-context few-shot learning results, setting a new state of the art on five tasks: VQAv2, VATEX, VizWiz, MSRVTTQA, and HatefulMemes. For example, on VQAv2, we observe improved results at 82.0%, outperforming our results achieved with 32-shot in-context learning (67.3%) as well as the previous state of the art (81.3%, Yan et al. [133]).

Although these fine-tuning results come at high computational cost relative to the previously presented in-context few-shot learning results – among other challenges like hyperparameter tuning – they further demonstrate the power of VLM pretraining for visual understanding even in the presence of large amounts of task-specific training data.

In some cases our results likely trail the state of the art due in part to the fact that we simply optimise log-likelihood and do not make use of common task-specific metric optimisation tricks, such as CIDEr optimisation [64, 90] for COCO captioning, and fine-tuning on dense annotations for VisDial [79]. For example, Murahari et al. [79] report a 10% relative improvement in NDCG on VisDial from such dense annotation fine-tuning.

B.2.3 Zero-shot performance of the pretrained contrastive model

A crucial part of our approach is the Vision Encoder, pretrained separately using contrastive learning and kept frozen when training Flamingo models. We report zero-shot image classification results on ImageNet, Kinetics700 and retrieval results on Flickr30K and COCO. The classification results are presented in Table 7 while the retrieval results are given in Table 9. For the retrieval tasks, our model outperforms the current state-of-the-art contrastive dual encoder approaches CLIP [85], ALIGN [50] and Florence [140]. However, we underperform the zero-shot state-of-the-art on Kinetics700 (CLIP) and the zero-shot state-of-the-art on ImageNet (BASIC). However, as noted earlier, BASIC [82] is particularly optimized for classification: it is trained on the JFT-3B [145] dataset which has images with labels rather than captions. We have noticed training on image and short text descriptions similar to labels significantly helps for ImageNet but is detrimental for retrieval benchmarks which require capturing rich scene descriptions instead. Since our goal is to use the Vision Encoder as a feature extractor for the Flamingo models in order to capture the whole scene and not just the main object, we favor retrieval metrics over classification ones. We provide more details about the contrastive pretraining in Appendix B.1.3.

Table 8: **Comparison to SotA when fine-tuning *Flamingo*.** We fine-tune *Flamingo* on all nine tasks where *Flamingo* was not SotA with few-shot learning. *Flamingo* sets a new SotA on five of these tasks sometimes even beating methods that resort to known performance optimization tricks such as model ensembling (on VQAv2, VATEX, VizWiz and HatefulMemes). Best numbers among the restricted SotA are in **bold**. Best numbers overall are underlined. Restricted SotA † only includes methods that use a single model (not ensembles) and do not directly optimise the test metric (no CIDEr optimisation).

Method	VQAv2		COCO	VATEX	VizWiz		MSRVTTQA	VisDial		YouCook2	TextVQA		HatefulMemes
	test-dev	test-std			test	test		test	valid		valid	valid	
Flamingo - 32 shots	67.6	-	113.8	65.1	49.8	-	31.0	56.8	-	86.8	36.0	-	70.0
SimVLM [124]	80.0	80.3	143.3	-	-	-	-	-	-	-	-	-	-
OFA [119]	79.9	80.0	<u>149.6</u>	-	-	-	-	-	-	-	-	-	-
Florence [140]	80.2	80.4	-	-	-	-	-	-	-	-	-	-	-
Flamingo Fine-tuned	82.0	82.1	138.1	84.2	65.7	65.4	47.4	61.8	59.7	118.6	57.1	54.1	86.6
Restricted SotA †	80.2	80.4	143.3	76.3	-	-	46.8	75.2	74.5	138.7	54.7	73.7	79.1
[140]	[140]	[124]	[153]	-	-	-	[51]	[79]	[79]	[132]	[137]	[84]	[62]
Unrestricted SotA	81.3	81.3	<u>149.6</u>	81.4	57.2	60.6	-	-	<u>75.4</u>	-	-	-	84.6
[133]	[133]	[119]	[153]	[65]	[65]	-	-	-	[123]	-	-	-	[152]

	Flickr30K						COCO					
	image-to-text			text-to-image			image-to-text			text-to-image		
	R@1	R@5	R@10									
Florence [140]	90.9	99.1	-	76.7	93.6	-	64.7	85.9	-	47.2	71.4	-
ALIGN [50]	88.6	98.7	99.7	75.7	93.8	96.8	58.6	83.0	89.7	45.6	69.8	78.6
CLIP [85]	88.0	98.7	99.4	68.7	90.6	95.2	58.4	81.5	88.1	37.7	62.4	72.2
Ours	89.3	98.8	99.7	79.5	95.3	97.9	65.9	87.3	92.9	48.0	73.3	82.1

Table 9: **Zero-shot contrastive pretraining evaluation.** Zero-shot image-text retrieval evaluation of our pretrained contrastive model compared to the state-of-the-art dual encoder contrastive models.

Ablated setting	Flamingo 3B value	Changed value	Param. count ↓	Step time ↓	COCO CIDEr↑	OKVQA top1↑	VQAv2 top1↑	MSVDQA top1↑	VATEX CIDEr↑	Overall score↑
Flamingo 3B model (short training)										
(i) Resampler size	Medium	Small Large	3.1B 3.4B	1.58s 1.87s	81.1 84.4	40.4 42.2	54.1 54.4	36.0 35.1	50.2 51.4	67.9 69.0
(ii) Multi-Img att.	Only last	All previous	3.2B	1.74s	70.0	40.9	52.0	32.1	46.8	63.5
(iii) p_{next}	0.5	0.0 1.0	3.2B 3.2B	1.74s 1.74s	85.0 81.3	41.6 43.3	55.2 55.6	36.7 36.8	50.6 52.7	69.6 70.4
(iv) LM pretraining	MassiveText	C4	3.2B	1.74s	81.3	34.4	47.1	60.6	53.9	62.8
(v) Freezing Vision	✓	✗ (random init) ✗ (pretrained)	3.2B 3.2B	4.70s* 4.70s*	74.5 83.5	41.6 40.6	52.7 55.1	31.4 34.6	35.8 50.7	61.4 68.1
(vi) Co-train LM on MassiveText	✗	✓ (random init) ✓ (pretrained)	3.2B 3.2B	5.34s* 5.34s*	69.3 83.0	29.9 42.5	46.1 53.3	28.1 35.1	45.5 51.1	55.9 68.6
(vii) Dataset and Vision encoder	M3W+ITP+VTP and NFNetF6	LAION400M and CLIP M3W+LAION400M+VTP and CLIP	3.1B 3.1B	0.86s 1.58s	61.4 76.3	37.9 41.5	50.9 53.4	27.9 32.5	29.7 46.1	54.7 64.9

Table 10: **Additional ablation studies.** Each row in this ablation study table should be compared to the baseline Flamingo run reported at the top of the table. The step time measures the time spent to perform gradient updates on all training datasets. (*): Due to higher memory usage, these models were trained using four times more TPU chips. The obtained accumulation step time was therefore multiplied by four.

B.3 Extended ablation studies

B.3.1 Flamingo

Ablation study experimental setup. As in Table 10, we report per-task results and the Overall score (see Section 3.3) for *Flamingo-3B* on the *validation* subsets of the 5 DEV multimodal benchmarks with 4 shots in Table 10. We perform the ablation using batch size of 256 for *M3W*, 512 for ALIGN, 512 for LTIP and 64 for VTP. Models are trained for 1 million gradient steps (meaning 250,000 gradient updates, for the base model as we accumulate gradients over four datasets).

Resampler size. We further investigate the architectural design of the Resampler in row (i) of Table 10. We ablate the size of our Resampler with three options: Small, Medium (default value for all Flamingo models), and Large. We see that the best performance is achieved with a medium size Resampler. Moreover, when scaled together with the frozen LM, we observed that increasing the size of the Perceiver Resampler lead to unstable training. We thus made a conservative choice to keep the same medium Resampler size for all our Flamingo models.

Effect of how many images are cross-attended to. In the interleaved image-text scenario, we ablate whether the model can only attend to the single most recent previous image, or to all the previous images (row (ii) of Table 10). We can see that the single image case leads to significantly better results (7.2% better in the overall score). One potential explanation is that when attending to all previous images, there is no explicit way of disambiguating between different images in the cross-attention inputs. Nonetheless, recent work has shown that such disambiguation is still possible implicitly through the causal attention mechanism [36]. We also explored more explicit ways to enable this while attending to all previous images by modifying the image tags to include an index (<image 1>, <image 2>, etc.) and/or learning absolute index embeddings added to the cross-attention features for each image. These strategies were not as robust as our method when the number of images per sequence changes between training and test time. Such a property is desirable

to reduce the number of images per sequence during training for better efficiency (we use $N = 5$ at training time) while still generalizing to many images for few-shot evaluation (we go up to $N = 32$ at test time). For these reasons, we keep the single image cross-attention strategy for the Flamingo models. Note that while the model cannot explicitly attend to all previous images due to this masking strategy, it can still implicitly attend to them from the language-only self-attention that propagates all previous images’ features via the previous text tokens.

M3W image placement data augmentation. Given a webpage, we don’t know in advance if the text of the page will mention the previous or the next image in the two-dimensional layout of the page DOM. For this reason, we explore a data augmentation on *M3W* controlled by p_{next} which indicates whether a given text token attends to the previous or the next image (see more details in Appendix A.3.2). The default value $p_{next} = \frac{1}{2}$ means that for each webpage sampled, we decide uniformly at random whether the model attends to the previous or next image. $p_{next} = 0$ means the model always attends to the previous image while $p_{next} = 1$ means the model always attends to the following image. The results (row (iii) of Table 10) show that using this randomization is beneficial.

Language model pretraining. To measure the importance of text pretraining, we compare the performance of using a frozen decoder-only Transformer either pretrained on MassiveText (our main model) or pretrained on the C4 dataset [87] (row (iv) of Table 10). Using the C4 dataset (which is smaller and less filtered than MassiveText) for training leads to a significant loss in performance (-7.9% overall). We note that the performance notably decreases for tasks that involve more language understanding such as visual question-answering tasks (OKVQA, VQAv2 and MSVDQA) while it remains on par for tasks that do not require as much language understanding (COCO, VATEX). This highlights the importance of pretraining the LM on a high-quality text-only dataset.

Freezing the vision encoder. During Flamingo training, we freeze the pretrained components (Vision Encoder and LM layers) while training newly added components from scratch. We ablate in (v) of Table 10 this freezing decision by training the Vision Encoder weights either from scratch or initialized with the contrastive vision-language task. If trained from scratch, we observe that the performance decreases by a large margin of -9.3% . Starting from pretrained weights still leads to a drop in performance of -2.6% while also increasing the compute cost of the training.

Alternative to freezing the LM by co-training on MassiveText. Another approach for preventing catastrophic forgetting is to co-train on MassiveText [86], the dataset that was used to pretrain the language model. Specifically, we add MassiveText to the training mixture, with a weight λ_m of 1.0 (best performing after a small grid search), using a sequence length of 2048 and the exact same setting as the pretraining of Chinchilla [42] for computing the text-only training loss. In order to co-train on MassiveText, we need to unfreeze the language model but we keep the vision encoder frozen. We perform two ablations in row (vi) of Table 10: starting from a pretrained language model (with a learning rate multiplier of 0.1 of the LM weights) versus initializing from scratch (with the same learning rate everywhere). In both cases, the overall scores are worse than our baseline which starts from the language model, pretrained on MassiveText, and is kept frozen throughout training. This indicates that the strategy of freezing the language model to avoid catastrophic forgetting is beneficial. Even more importantly, freezing the LM is computationally cheaper as no gradient updates of the LM weights are required and we do not need to train on an additional dataset. This computational argument is even more relevant for our largest model, *Flamingo-80B*, where we freeze almost 90% of the overall weights.

Additional experiments using the LAION400M dataset. In order to provide reference numbers that are more easily reproducible using publicly available datasets and network weights we also provide two additional ablations using the CLIP ViT L-14 weights [85] and the LAION400M dataset [96] in rows (vii) of Table 10.

B.3.2 Dataset mixing strategies for the contrastive pretraining

One key to achieving strong results was the inclusion of our new dataset LTIP alongside ALIGN for training. Despite being a smaller dataset ALIGN by a factor of 6, a contrastive model trained on only LTIP outperforms one trained only on ALIGN on our evaluation metrics, suggesting that dataset quality may be more important than scale in the regimes in which we operate. We also find that a

Dataset	Combination strategy	ImageNet accuracy top-1	COCO					
			image-to-text			text-to-image		
			R@1	R@5	R@10	R@1	R@5	R@10
LTIP	None	40.8	38.6	66.4	76.4	31.1	57.4	68.4
ALIGN	None	35.2	32.2	58.9	70.6	23.7	47.7	59.4
LTIP + ALIGN	Accumulation	45.6	42.3	68.3	78.4	31.5	58.3	69.0
LTIP + ALIGN	Data merged	38.6	36.9	65.8	76.5	15.2	40.8	55.7
LTIP + ALIGN	Round-robin	41.2	40.1	66.7	77.6	29.2	55.1	66.6

Table 11: **Effect of contrastive pretraining datasets and combination strategies.** The first two rows show the effect of training a small model on LTIP and ALIGN only; the final three show the results of a small model trained on combinations of these datasets, comparing different combination strategies.

model trained on both ALIGN and LTIP outperforms those trained on the two datasets individually and that how the datasets are combined is important.

To demonstrate this, we train a small model with an NFNet-F0 vision encoder, BERT-mini language encoder and batch size 2048 for 1 million gradient-calculation steps on ALIGN, LTIP and a mixture of the two. The results are presented in Table 11. It shows the results of training models on the combined datasets using three different merging regimes:

- Data merged: Batches are constructed by merging examples from each dataset into one batch.
- Round-robin: We alternate batches of each dataset, updating the parameters on each batch.
- Accumulation: We compute a gradient on a batch from each dataset. These gradients are then weighted and summed and use to update the parameters.

Across all evaluation metrics, we find that the Accumulation method outperforms other methods of combining the datasets. Although the LTIP dataset is $5 \times$ smaller than the ALIGN dataset, this ablation study suggests that the quality of the training data can be more important than its abundance.

C Qualitative results

In addition to the samples in Figure 1, in this section we provide selected samples covering different interaction modalities in Figures 10, 11, and 12. Unlike the quantitative benchmark results which use beam search with a beam width of 3 for decoding, all qualitative results presented in this section use greedy decoding for faster sampling.

Figure 10 shows the simplest form of interaction where a single image is provided followed by a text prompt either in the form of a question or the start of a caption. Even though the model is not trained specifically for the question and answer format, the capabilities of the pretrained language model allows this adaptation. In many of these examples, *Flamingo* can do at least one step of implicit inference. Some of the objects are not named in the prompt but their properties are queried directly. Based on its visual input, the model manages to recall the knowledge relevant to the referred object and thus produces the correct answer. Vision networks trained contrastively have been shown to learn character recognition capabilities [85]. We observe that *Flamingo* preserves this capability in the full model, in some cases for text that is rather small with respect to the size of the image.

Since our model can accept inputs in the form of arbitrary sequences of visuals and language, we test its abilities to hold an extended dialogue with interleaved images and text. Figure 11 shows some samples which are generated by prompting the model with a brief dialogue (Appendix B.1.6) followed by user interaction including image insertions. Even after several rounds of interaction *Flamingo* can still successfully attend to the image and reply to questions that can not be guessed by language alone. We observe that multiple images can be separately attended: simple comparisons and inferences are handled properly.

Lastly, we investigated similar capabilities with video inputs as they present some extra challenges compared to images. Figure 12 shows some selected samples. As seen in the figure, in some cases

Flamingo can successfully integrate information from multiple frames (e.g., videos scanning through a scene or text) and answer questions involving temporal understanding (e.g., in the last example, with the word “after”).

D Discussion

D.1 Limitations, failure cases and opportunities

Here, we describe some limitations and failure cases of our models, as well as opportunities for further improving our models and extending their abilities.

Classification performance. Although our visual language models have important advantages over contrastive models (e.g., few-shot learning and open-ended generation capabilities), their performance lags behind that of contrastive models on classification tasks. We believe this is because the contrastive training objective directly optimizes for text-image retrieval, and in practice, the evaluation procedure for classification can be thought of as a special case of image-to-text retrieval [85]. This is not the case for the language modeling objective we use to train our visual language models and this may contribute to the observed performance gap on classification tasks. In particular, Zhao et al. [148] have shown that language models suffer from various biases arising from the training data distribution, the set of samples used in the prompt, and their order. They also show that such issues can be mitigated with calibration techniques, provided one can assume a certain prior distribution (e.g., uniform) over the label space. This assumption doesn’t hold in general, and further research is needed to develop techniques to address these issues in the few-shot setting. More generally, seeking objectives, architectures, or evaluation procedures that could bridge the gap between these two classes of models is a promising research direction.

Legacies of language models. Our models build on powerful pretrained causal language models, and as a side effect, directly inherit their weaknesses. For instance, causal modeling of the conditioning inputs is strictly less expressive than bidirectional modeling. In this direction, recent work has shown that non-causal masked language modeling adaptation [120] followed by multitask fine-tuning [95, 125, 131] can efficiently improve the zero-shot performance of causal decoder-only language models. Furthermore, transformer-based language models tend to generalize poorly to test sequences significantly longer than the training ones [83]. In settings where the expected text output is too long, the ability of the models to leverage enough shots for few-shot learning can be affected. For instance, for the VisDial dataset [20], a single shot consists of an image followed by a long dialogue composed of 21 different sentences. A sequence of 32 VisDial shots is thus composed of at least $32 \times 21 = 672$ sentences, which in practice means that the prompt length ranges from 4096 to 8192 tokens. This is significantly longer than the maximum sequence length (2048) our LMs have been trained on [42]. To this end, we have capped our reported results on VisDial at 16 shots. On another note, while our ablations demonstrate the importance of the language model priors inherited from frozen language models, we suspect that they may play a role in occasional hallucinations and ungrounded guesses observed in open-ended dialogue settings. We provide and analyze examples of such behaviours in Figure 13. Finally, language modeling suffers from poor sample efficiency during pretraining [11]. Mitigating this issue has the potential to greatly accelerate progress in the field, by improving turnaround of large-scale training runs and in turn increasing the feasibility of more systematic exploration of design decisions at larger scales. Further discussion on typical weaknesses observed for large LMs can be found in [11, 86].

Trade-offs of few-shot learning methods. In the paper, we use in-context learning as our “go-to” few-shot learning method (see Section 2.5). This method has notable advantages over gradient-based approaches such as fine-tuning. Indeed, in-context learning requires almost no hyperparameter tuning, works reasonably well in the very low data regime (dozens of examples), and only requires inference, simplifying deployment. In contrast, gradient-based approaches require carefully tuned design choices to avoid overfitting (either by proper learning rate schedule or architecture design [43]) and often need more data (thousands) to work well. This motivated our focus on in-context learning; however, this approach also has drawbacks we discuss next.

Inference compute cost. The compute cost of in-context learning with transformer models scales linearly with the number of shots if one can reuse the few-shot prompt for multiple query samples

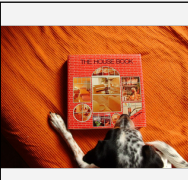
<p>Input Prompt</p>  <p>Question: What do you think the capacities of these are? Answer:</p>	 <p>Question: What is odd about this image? Explain why it is unusual. Answer:</p>	 <p>Question: What country is this? Why do you think so? Answer:</p>
<p>Completion</p> <p>The floppy disk is 1.44MB and the CD is 700MB.</p>	<p>The image is odd because the elephant is in the back of the truck. It is unusual because elephants are not usually transported in the back of a truck.</p>	<p>It is Canada. I think so because the flag is the Canadian flag.</p>
<p>Input Prompt</p>  <p>Question: What nutrients is the fruit in the image rich in? Answer:</p>	 <p>Question: What is the purpose of this? Answer:</p>	 <p>Question: What season is this? Explain why. Answer:</p>
<p>Completion</p> <p>Vitamin C, potassium, and fiber.</p>	<p>To keep the mosquitoes out of the bed.</p>	<p>This is winter season. The Christmas tree and the presents are the main reasons why it is winter.</p>
<p>Input Prompt</p>  <p>Question: What is the title of the book? Answer:</p>	 <p>The ingredients of this dish are</p>	 <p>The soundtrack includes</p>
<p>Completion</p> <p>The House Book.</p>	<p>: beef, potatoes, carrots, broccoli, and lemon.</p>	<p>the songs "Let It Go" and "For the First Time in Forever" by Tony Award® winner Idina Menzel, who plays Elsa [...]</p>

Figure 10: **Selected single image samples.** Gray boxes are user input and the pink boxes are *Flamingo* output.

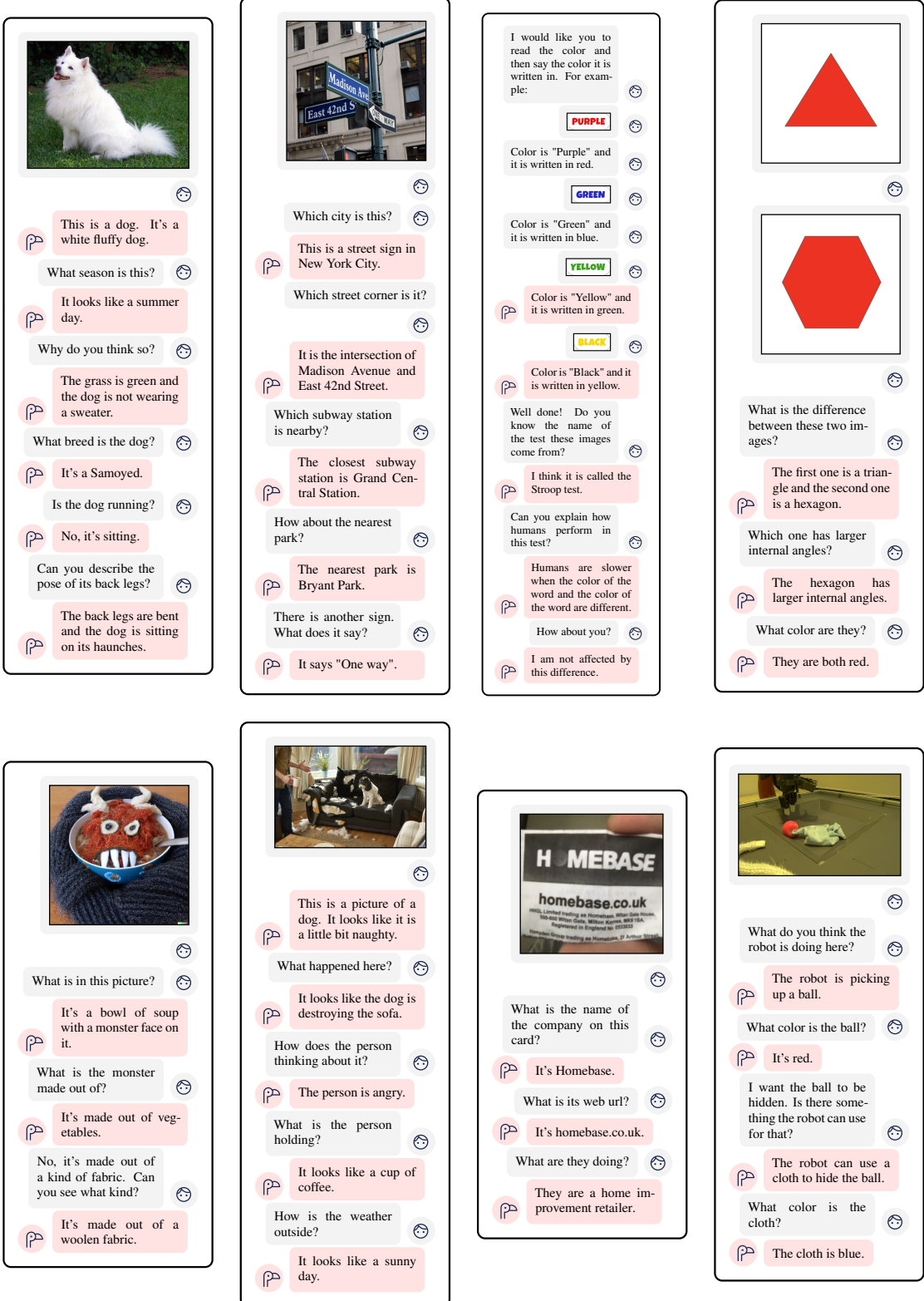


Figure 11: **Selected dialogue samples.** Gray boxes are user input and the pink boxes are *Flamingo* output. For dialogue, *Flamingo* is provided with a custom prompt (hidden from the visualization but shown in Appendix B.1.6) containing a dialogue with 3 corresponding images, but it is not fine-tuned for dialogue in any other way.



Figure 12: **Selected video samples.** These are all of the frames the model sees. (Best viewed with zoom.)

(by caching the keys and values) and quadratically otherwise. In contrast, gradient-based few-shot learning approaches [43] have constant complexity with respect to the number of shots during inference.

Prompt sensitivity. In-context learning has also been shown to be disconcertingly sensitive to various aspects of the demonstrations, such as the order of the samples [148] or their format.

Leveraging more shots. When using in-context learning, performance plateaus rapidly as the number of few-shot samples increases beyond 32. This proves a striking contrast with typical gradient-based methods, for which the amount of correctly paired training data is a critical factor for performance. We note that RICES (Retrieval In-Context Example Selection [136] described in Appendix A.2) effectively mitigates this issue for classification tasks (Appendix B.2.1), but still faces similar issues beyond a small number of example per class.

Task location. Recent work on understanding what makes in-context learning effective sheds some light on a possible explanation for why more shots do not always help [76, 92]. In more detail, Brown et al. [11] raise the question of whether in-context learning actually “learns” new tasks at inference time based on the provided input-output mappings, or simply recognizes and identifies tasks learned during training. On this question, the findings of Reynolds and McDonell [92] suggest that the latter is the key driver of performance across diverse settings, and refer it as *task location*. Similarly, Min et al. [76] show that the mapping from input to output generally has limited impact on few-shot performance, as opposed to specifying the overall format of the examples. In line with these findings, we also observe non-trivial zero-shot performance using prompt without any images, hence also highlighting that the format of the task matters significantly. Intuitively, a handful of samples may often be enough to perform task location well, but the model may generally not be able to leverage further samples at inference time to refine its behaviour.

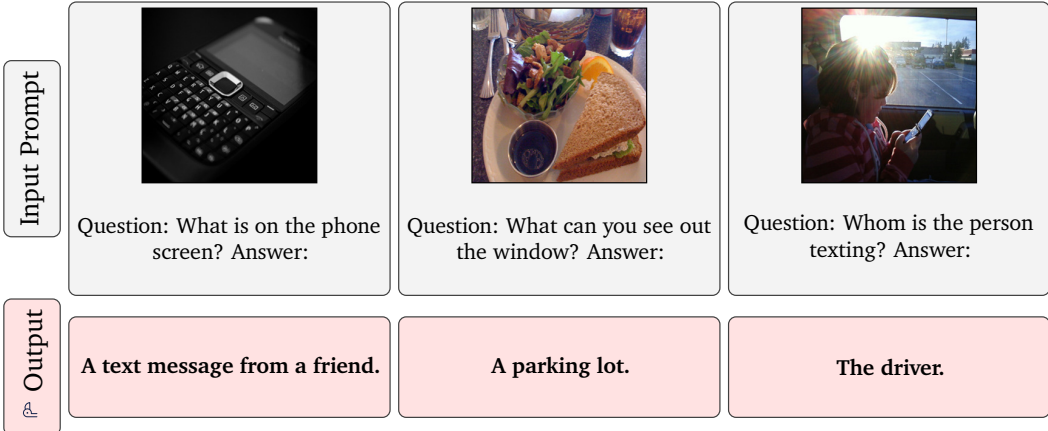


Figure 13: **Hallucinations and ungrounded guesses in open-ended visual question answering.** *Left:* The model occasionally hallucinates by producing answers that seem likely given the text only, but are wrong given the image as additional input. *Middle:* Similar hallucinations can be provoked by adversarially prompting the model with an irrelevant question. *Right:* A more common pitfall arises when the model makes ungrounded guesses when the answer cannot be determined based on the inputs. Few-shot examples and more sophisticated prompt design may be used to mitigate these issues. More broadly, addressing these issues is an important research direction towards improving our models’ applications in open-ended visual dialogue settings.

In summary, there is no “golden” few-shot method that would work well in all scenarios. In particular, the best choice of few-shot learning approach strongly depends on characteristics of the application, an important one being the number of annotated samples. On this point, in our work, we demonstrate that in-context learning is highly effective in the data-starved regime (32 samples or fewer). There may be opportunities to combine different methods to leverage their complementary benefits, in particular when targeting less data-constrained data regimes (e.g., hundreds of samples).

Extending the visual and text interface. Natural language is a powerful and versatile input/output interface to provide descriptions of visual tasks to the model and generate outputs or estimate conditional likelihoods over possible outputs. However, it may be a cumbersome interface for tasks that involve conditioning on or predicting more structured outputs such as bounding boxes (or their temporal and spatio-temporal counterparts); as well as making spatially (or temporally and spatio-temporally) dense predictions. Furthermore, some vision tasks, such as predicting optical flow, involve predicting in continuous space, which is not something our model is designed to handle out of the box. Finally, one may consider additional modalities besides vision that may be complementary, such as audio. All of these directions have the potential to extend the range of tasks that our models can handle; and even improve performance on the ones we focus on, thanks to synergies between the corresponding abilities.

Scaling laws for vision-language models. In this work, we scale Flamingo models up to 80B parameters and provide some initial insights on their scaling behaviour across evaluation benchmarks, summarized in Figure 2. In the language space, an important line of work has focused on establishing scaling laws for language models [42, 53]. In the vision domain, Zhai et al. [145] take a step in this direction. Similar efforts have yet to be made for vision-language models, including contrastive models, as well as visual language models such as the ones we propose. While language modeling scaling law research has focused on perplexity as the golden metric, we speculate that it may be more directly useful for our purposes to establish such trends in terms of aggregate downstream evaluation task performance.

D.2 Benefits, risks and mitigation strategies

D.2.1 Benefits

Accessibility. A system like Flamingo offers a number of potential societal benefits, some of which we will discuss in this section. Broadly, the fact that Flamingo is capable of task generalisation makes it suitable for use cases that have not been the focus of vision research historically. Typical vision systems are trained to solve a particular problem by training on large databases of manually annotated task-specific examples, making them poorly suited for applications outside of the narrow use cases for which they were deliberately trained. On the other hand, Flamingo is trained in a minimally constrained setting, endowing it with strong few-shot task induction capabilities. As we’ve shown in our qualitative examples (Appendix C), Flamingo can also be used through a “chat”-like interface for open-ended dialogue. Such capabilities could enable non-expert end users to apply models like Flamingo even to low-resource problems for which little to no task-specific training data has been collected, and where queries might be posed in a variety of formats and writing styles. In this direction, we have shown that *Flamingo* achieves strong performance on the VizWiz challenge¹, which promotes visual recognition technologies to assist visually impaired people. A dialogue interface could also promote better understanding and interpretability of visual language models. It could help highlight issues with bias, fairness, and toxicity the model may pick up on from the training data. Overall, we believe that Flamingo represents an important step towards making state-of-the-art visual recognition technology more broadly accessible and useful for many diverse applications.

Model recycling. From a modeling perspective, although Flamingo is computationally expensive to train, it importantly leverages pretrained frozen language models and visual encoders. We demonstrated that new modalities can be introduced into frozen models, thereby avoiding expensive retraining. As such models continue to grow in size and computational demands, “recycling” them will become increasingly important from an environmental perspective (as well as a practical one), as described in Larochelle [55] and explored in Strubell et al. [105] for language models. We hope such results may inspire further research into how existing models can be repurposed efficiently rather than trained from scratch.

D.2.2 Risks and mitigation strategies

This section provides some early investigations of the potential risks of models like Flamingo. This study is preliminary and we foresee that further research efforts should be undertaken to better assess those risks. We also discuss potential mitigation strategies towards safely deploying these models. Note that as explained in our Model Card [77] in Appendix E, this model was developed for research purposes only and should not be used in specific applications before proper risk analyses are conducted and mitigation strategies are explored.

By construction, *Flamingo* inherits the risks of Large LMs. Recall that a large part of our model is obtained by freezing the weights of an existing language model [42]. In particular, if provided with no images *Flamingo* falls back to language model behavior. As such *Flamingo* is exposed to the same risks of large language models: it can output potentially offensive language, propagate social biases and stereotypes, as well as leaking private information [126]. In particular, we refer to the analysis presented in the Chinchilla paper (Hoffmann et al. [42], Section 4.2.7) in terms of gender bias on the Winogender dataset [93] which demonstrate that even though this model is less biased towards gender than previous models [86], gender biases are still present. In terms of unprompted toxicity, we also refer to the analysis from Chinchilla [42] which highlights that overall the propensity of the model to produce toxic outputs when not prompted to do so is rather low, as measured by computing the *PerspectiveAPI* toxicity score on 25,000 samples. Weidinger et al. [126] detail possible long-term mitigation strategies for these risks. They include social or public policy interventions, such as the creation of regulatory frameworks and guidelines; careful product design, for instance relating to user interface decisions; and research at the intersection between AI Ethics and NLP, such as building better benchmarks and improving mitigation strategies. In the short term, effective approaches include relying on prompting to mitigate any biases and harmful outputs [86]. Next, we explore the additional risks incurred by Flamingo’s additional visual input capabilities.

¹<https://vizwiz.org/>

	female - male = Δ	CIDEr difference darker - lighter = Δ	CIDEr overall
AoANet [46]	-	+0.0019	1.198
Oscar [61]	-	+0.0030	1.278
<i>Flamingo</i> , 0 shot	$0.899 - 0.870 = +0.029 (p = 0.52)$	$0.955 - 0.864 = +0.091 (p = 0.25)$	0.843
<i>Flamingo</i> , 32 shots	$1.172 - 1.142 = +0.030 (p = 0.54)$	$1.128 - 1.152 = -0.025 (p = 0.76)$	1.138

Table 12: **Bias evaluation of *Flamingo* for COCO captioning.** We report results on the COCO dataset splits over gender and skin tone provided by Zhao et al. [147].

Gender and racial biases when prompted with images. Previous work has studied biases that exist in captioning systems [37, 147]. Such modeling biases can result in real-world harms if deployed without care. For AI systems to be useful to society as a whole, their performance should not depend on the perceived skin tone or gender of the subjects – they should work equally well for all populations. However, current automatic vision system performance has been reported to vary with race, gender or when applied across different demographics and geographic regions [12, 21, 97]. As a preliminary study assessing how Flamingo’s performance varies between populations, we follow the study proposed in Zhao et al. [147] and report how the captioning performance of our model varies on COCO as a function of gender and race. Note that we use a different evaluation protocol from the one proposed by Zhao et al. [147]; in that work, they measure results across 5 pretrained models and compute confidence intervals across aggregated per-model scores. Here, we have just one copy of our model (due to its high training cost), and we instead perform statistical tests on the per-sample CIDEr scores across the splits from Zhao et al. [147]. We report the results in Table 12.

Overall, when comparing the CIDEr scores aggregated among images labeled as *female* versus *male*, as well as when comparing *darker skin* versus *lighter skin*, we find there are no statistically significant differences in the per-sample CIDEr scores. To compare the two sets of samples, we use a two-tailed *t*-test with unequal variance, and among the four comparisons considered, the lowest *p*-value we find is *p* = 0.25, well above typical statistical significance thresholds (e.g. a common rejection threshold might be *p* < α = 0.05). This implies that the differences in scores are indistinguishable from random variation under the null hypothesis that the mean scores are equal. We note that a failure to reject the null hypothesis and demonstrate a significant difference does not imply that there are no significant differences; it is possible that a difference exists that could be demonstrated with larger sample sizes, for example. However, these preliminary results are nonetheless encouraging.

Toxicity when prompted with images. We also evaluate the toxicity of *Flamingo* using the *Perspective API*² to evaluate the toxicity of the model’s generated captions when prompted with images from the COCO test set. We observe that some captions are labelled as potentially toxic by the classifier; however, when examining them manually, we do not observe any clear toxicity – output captions are appropriate for the images provided. Overall, based on our own experiences interacting with the system throughout the course of the project, we have not observed toxic outputs when given “safe-for-work” imagery. However this does not mean the model is incapable of producing toxic outputs, especially if probed with “not-safe-for-work” images and/or toxic text. A more thorough exploration and study would be needed if such a model were put in production.

Applying Flamingo for mitigation strategies. Thanks to its ability to rapidly adapt in low-resource settings, *Flamingo* could itself be applied in addressing some of the issues described above. For instance, following Thoppilan et al. [111], adequately conditioned or fine-tuned Flamingo models could be used for filtering purposes of toxic or harmful samples in the training data. In their work, they observe significant improvements relating to safety and quality when fine-tuning on the resulting data. Furthermore, during evaluation, such adapted models could be used to down-rank or exclude outputs that might be classified as offensive, promoting social biases and stereotypes or leaking private information, thus accelerating progress in this direction even for low-resource tasks. Our results on the HatefulMemes benchmark represent a promising step in this direction. Recent work in the language modeling space has also shown success in training an LM to play the role of a “red team” and generate test cases, so as to automatically find cases where another target LM behaves in a harmful way [81]. A similar approach could be derived for our setting. Enabling the model to

²<https://perspectiveapi.com/>

support outputs with reference to particular locations within the visual inputs, or to external verified quotes is also an interesting direction [72, 111]. Finally, in Figure 11, we provide qualitative examples demonstrating that Flamingo can explain its own outputs, suggesting avenues to explainability and interpretability using the model’s text interface.

E Flamingo Model Card

We present a model card for Flamingo in Table 13, following the framework presented by Mitchell et al. [77].

Model Details	
Model Date	March 2022
Model Type	Transformer-based autoregressive language model, conditioned on visual features from a convnet-based encoder. Additional transformer-based cross-attention layers incorporate vision features into the language model’s text predictions. (See Section 2 for details.)
Intended Uses	
Primary Intended Uses	The primary use is research on visual language models (VLM), including: research on VLM applications like classification, captioning or visual question answering, understanding how strong VLMs can contribute to AGI, advancing fairness and safety research in the area of multimodal research, and understanding limitations of current large VLMs.
Out-of-Scope Uses	Uses of the model for visually conditioned language generation in harmful or deceitful settings. Broadly speaking, the model should not be used for downstream applications without further safety and fairness mitigations specific to each application.
Factors	
Card Prompts – Relevant Factor	Relevant factors include which language is used. Our model is trained on English data. Our model is designed for research. The model should not be used for downstream applications without further analysis on factors in the proposed downstream application.
Card Prompts – Evaluation Factors	<i>Flamingo</i> is based on Chinchilla (a large proportion of the weights of Chinchilla are used as this) and we refer to the analysis provided in [42, 86] for the language only component of this work. We refer to our study presented in Appendix D.2.2 for a toxicity analysis when the model is conditioned on an image.
Metrics	

Model Performance Measures

We principally focus on the model’s ability to predict relevant language when given an image. For that we used a total of 18 different benchmarks described in Appendix B.1.4 spanning various vision and language tasks such as classification (ImageNet, Kinetics700, HatefulMemes), image and video captioning (COCO, VATEX, Flickr30K, YouCook2, RareAct), visual question answering (OKVQA, VizWiz, TextVQA, VQAv2, MSRVTTQA, MSVDQA, iVQA, STAR, NextQA) and visual dialog (VisDiag). This was tested either in an open ended setting where *Flamingo* generate language and we compare the outputs with the ground truth or in a close ended setting where we directly score various outcomes using the likelihood of the model.

Decision thresholds	N/A
Approaches to Uncertainty and Variability	Due to the costs of training <i>Flamingo</i> , we cannot train it multiple times. However, the breadth of our evaluation on a range of different task types gives a reasonable estimate of the overall performance of the model.

Evaluation Data

Datasets	See Table 6 for a detailed list.
Motivation	We chose our evaluation datasets to span an important range of vision and language tasks to correctly assess the ability of <i>Flamingo</i> to produce relevant text given an image.
Preprocessing	Input text is tokenized using a SentencePiece tokenizer with a vocabulary size of 32,000. Images are processed so that their mean and variance are 0 and 1 respectively.

Training Data

See [50], the Datasheet in Appendix F.1, Appendix F.2.1, Appendix F.2.2

Quantitative Analyses

Unitary Results	<i>Flamingo</i> sets a new state of the art in few-shot learning on a wide range of open-ended vision and language tasks. On the 16 tasks we consider, Flamingo also surpasses the fine-tuned state-of-art in 6 of the cases despite using orders of magnitude less task-specific training data. We refer to Section 3 for the full details of our quantitative study.
Intersectional Results	We did not investigate intersectional biases.

Ethical Considerations

Data	The data is sourced from a variety of sources, some of it from web content. Sexually explicit content is filtered out, but the dataset does include racist, sexist or otherwise harmful content.
Human Life	The model is not intended to inform decisions about matters central to human life or flourishing.

Mitigations	Apart from removing sexual explicit content we did not filter out toxic content, following the rationale of Rae et al. [86]. More work is needed on mitigation approaches to toxic content and other types of risks associated with language models, such as those discussed in Weidinger et al. [126].
Risks and Harms	The data is collected from the internet, and thus undoubtedly toxic and biased content is included in our training dataset. Furthermore, it is likely that personal information is also in the dataset that has been used to train our models. We defer to the more detailed discussion in Weidinger et al. [126].
Use Cases	Especially fraught use cases include the generation of factually incorrect information with the intent of distributing it or using the model to generate racist, sexist or otherwise toxic text with harmful intent. Many more use cases that could cause harm exist. Such applications to malicious use are discussed in detail in Weidinger et al. [126].

Table 13: **Flamingo Model Card.** We follow the framework presented in Mitchell et al. [77].

F Datasheets

F.1 M3W dataset

We follow the framework defined by Gebru et al. [30] and provide the datasheet for *M3W* in Table 14.

Motivation	
For what purpose was the dataset created? Who created the dataset? Who funded the creation of the dataset?	The dataset was created for pre-training vision-language models and was created by researchers and engineers.
Any other comments?	None.
Composition	
What do the instances that comprise the dataset represent (e.g., documents, photos, people, countries)?	All instances of the dataset are documents from the web containing interleaved text and images.
How many instances are there in total (of each type, if appropriate)?	There are 43.3M instances (documents) in total, with a total of 185M images and 182 GB of text.
Does the dataset contain all possible instances or is it a sample (not necessarily random) of instances from a larger set?	The dataset is a sample from a larger set.
What data does each instance consist of?	Each instance is made up of a sequence of UTF-8 bytes encoding the document’s text, as well as a sequence of integers indicating the positions of images in the text, and the images themselves in compressed format (see Section 2.4).
Is there a label or target associated with each instance?	No, there are no labels associated with each instance.

Is any information missing from individual instances?	No.
Are relationships between individual instances made explicit?	There are no relationships between the different instances in the dataset.
Are there recommended data splits?	We use random splits for the training and development sets.
Are there any errors, sources of noise, or redundancies in the dataset?	There is significant redundancy at the sub-document level.
Is the dataset self-contained, or does it link to or otherwise rely on external resources?	The dataset is self-contained.
Does the dataset contain data that might be considered confidential?	No.
Does the dataset contain data that, if viewed directly, might be offensive, insulting, threatening, or might otherwise cause anxiety?	The dataset likely contains some data that might be considered offensive, insulting or threatening, as such data is prevalent on the web. We do not try to filter out such content, with the exception of explicit content, which we identify using dedicated filter.

Collection Process

How was the data associated with each instance acquired?	The data is available publicly on the web.
What mechanisms or procedures were used to collect the data?	The data was collected using a variety of software programs to extract and clean the raw text and images.
If the dataset is a sample from a larger set, what was the sampling strategy?	We randomly subsample documents.
Over what timeframe was the data collected?	The dataset was collected over a period of several months in 2021. We do not filter the sources based on creation date.
Were any ethical review processes conducted?	No.

Preprocessing/cleaning/labeling

Was any preprocessing/Cleaning/Labeling of the data done (e.g., discretization or bucketing, tokenization, part-of-speech tagging, SIFT feature extraction, removal of instances, processing of missing values)?	Yes — the pre-processing details are discussed in Appendix A.3.1.
Is the software used to preprocess/-clean/label the instances available?	No.

Uses

Has the dataset been used for any tasks already?	Yes, we use the dataset for pre-training multimodal language and vision models.
Is there a repository that links to any or all papers or systems that use the dataset?	No, the dataset has only been used to train the models in this paper.

What (other) tasks could the dataset be used for?	We do not foresee other usages of the dataset at this stage.
Is there anything about the composition of the dataset or the way it was collected and preprocessed/cleaned/labeled that might impact future uses?	The dataset is static and thus will become progressively more “stale”. For example, it will not reflect new language and norms that evolve over time. However, due to the nature of the dataset it is relatively cheap to collect an up-to-date version.
Are there tasks for which the dataset should not be used?	The dataset described in this paper contains English language text almost exclusively and therefore should not be used for training models intended to have multilingual capabilities.

Distribution

Will the dataset be distributed to third parties outside of the entity (e.g., company, institution, organization) on behalf of which the dataset was created?	No.
---	-----

Table 14: **M3W Datasheet**. We follow the framework as presented by Gebru et al. [30].

F.2 Image and video text pair datasets

F.2.1 Datasheet for LTIP

Motivation	
For what purpose was the dataset created? Who created the dataset? Who funded the creation of the dataset?	The dataset was created for pre-training vision-language models and was created by researchers and engineers.
Any other comments?	None.
Composition	
What do the instances that comprise the dataset represent (e.g., documents, photos, people, countries)?	All instances of the dataset are image-text pairs.
How many instances are there in total (of each type, if appropriate)?	The dataset contains 312M image-text pairs.
Does the dataset contain all possible instances or is it a sample (not necessarily random) of instances from a larger set?	The dataset is a sample from a larger set.
What data does each instance consist of?	Each instance is made up of a sequence of UTF-8 bytes encoding the document's text, and an image in compressed format (see Appendix A.3.3).
Is there a label or target associated with each instance?	No, there are no labels associated with each instance.
Is any information missing from individual instances?	No.
Are relationships between individual instances made explicit?	There are no relationships between the different instances in the dataset.
Are there recommended data splits?	We use random splits for the training and development sets.
Are there any errors, sources of noise, or redundancies in the dataset?	The data is relatively high quality but there is a chance that some instances are repeated multiple times.
Is the dataset self-contained, or does it link to or otherwise rely on external resources?	The dataset is self-contained.
Does the dataset contain data that might be considered confidential?	No.
Does the dataset contain data that, if viewed directly, might be offensive, insulting, threatening, or might otherwise cause anxiety?	The websites that were used for this dataset were carefully selected to avoid such content. However given the scale of the data it is possible that some data could be considered offensive or insulting.
Collection Process	
How was the data associated with each instance acquired?	The data is available publicly on the web.
What mechanisms or procedures were used to collect the data?	The data was collected using a variety of software programs to extract and clean the raw text and images.

If the dataset is a sample from a larger set, what was the sampling strategy?	N.A.
Over what timeframe was the data collected?	The dataset was collected over a period of several months in 2021. We do not filter the sources based on creation date.
Were any ethical review processes conducted?	No.

Preprocessing/cleaning/labeling

Was any preprocessing/Cleaning/Labeling of the data done (e.g., discretization or bucketing, tokenization, part-of-speech tagging, SIFT feature extraction, removal of instances, processing of missing values)?	Some automatic text formatting was applied to remove from the captions dates and locations that were not relevant to the training objective.
Is the software used to preprocess/-clean/label the instances available?	No.

Uses

Has the dataset been used for any tasks already?	Yes, we use the dataset for pre-training multimodal language and vision models.
Is there a repository that links to any or all papers or systems that use the dataset?	No, the dataset has only been used to train the models in this paper.
What (other) tasks could the dataset be used for?	We do not foresee other usages of the dataset at this stage.
Is there anything about the composition of the dataset or the way it was collected and preprocessed/-cleaned/labeled that might impact future uses?	The dataset is static and thus will become progressively more “stale”. For example, it will not reflect new language and norms that evolve over time. However, due to the nature of the dataset it is relatively cheap to collect an up-to-date version.
Are there tasks for which the dataset should not be used?	The dataset described in this paper contains English language text almost exclusively and therefore should not be used for training models intended to have multilingual capabilities.

Distribution

Will the dataset be distributed to third parties outside of the entity (e.g., company, institution, organization) on behalf of which the dataset was created?	No.
---	-----

Table 15: **LTIP Datasheet**. We follow the framework as presented by Gebru et al. [30].

F.2.2 Datasheet for VTP

Motivation	
For what purpose was the dataset created? Who created the dataset? Who funded the creation of the dataset?	The dataset was created for pre-training vision-language models and was created by researchers and engineers.
Any other comments?	None.
Composition	
What do the instances that comprise the dataset represent (e.g., documents, photos, people, countries)?	All instances of the dataset are video-text pairs.
How many instances are there in total (of each type, if appropriate)?	The dataset contains 27M video-text pairs.
Does the dataset contain all possible instances or is it a sample (not necessarily random) of instances from a larger set?	The dataset is a sample from a larger set.
What data does each instance consist of?	Each instance is made up of a sequence of UTF-8 bytes encoding the document's text, and a video in compressed format (see Appendix A.3.3).
Is there a label or target associated with each instance?	No, there are no labels associated with each instance.
Is any information missing from individual instances?	No.
Are relationships between individual instances made explicit?	There are no relationships between the different instances in the dataset.
Are there recommended data splits?	We use random splits for the training and development sets.
Are there any errors, sources of noise, or redundancies in the dataset?	The data is relatively high quality but there is a chance that some instances are repeated multiple times.
Is the dataset self-contained, or does it link to or otherwise rely on external resources?	The dataset is self-contained.
Does the dataset contain data that might be considered confidential?	No.
Does the dataset contain data that, if viewed directly, might be offensive, insulting, threatening, or might otherwise cause anxiety?	The websites that were used for this dataset were carefully selected to avoid such content. However given the scale of the data it is possible that some data could be considered offensive or insulting.
Collection Process	
How was the data associated with each instance acquired?	The data is available publicly on the web.
What mechanisms or procedures were used to collect the data?	The data was collected using a variety of software programs to extract and clean the raw text and videos.

If the dataset is a sample from a larger set, what was the sampling strategy?	N.A.
Over what timeframe was the data collected?	The dataset was collected over a period of several months in 2021. We do not filter the sources based on creation date.
Were any ethical review processes conducted?	No.

Preprocessing/cleaning/labeling

Was any preprocessing/Cleaning/Labeling of the data done (e.g., discretization or bucketing, tokenization, part-of-speech tagging, SIFT feature extraction, removal of instances, processing of missing values)?	Some automatic text formatting was applied to remove from the captions dates and locations that were not relevant to the training objective.
Is the software used to preprocess/-clean/label the instances available?	No.

Uses

Has the dataset been used for any tasks already?	Yes, we use the dataset for pre-training multimodal language and vision models.
Is there a repository that links to any or all papers or systems that use the dataset?	No, the dataset has only been used to train the models in this paper.
What (other) tasks could the dataset be used for?	We do not foresee other usages of the dataset at this stage.
Is there anything about the composition of the dataset or the way it was collected and preprocessed/-cleaned/labeled that might impact future uses?	The dataset is static and thus will become progressively more “stale”. For example, it will not reflect new language and norms that evolve over time. However, due to the nature of the dataset it is relatively cheap to collect an up-to-date version.
Are there tasks for which the dataset should not be used?	The dataset described in this paper contains English language text almost exclusively and therefore should not be used for training models intended to have multilingual capabilities.

Distribution

Will the dataset be distributed to third parties outside of the entity (e.g., company, institution, organization) on behalf of which the dataset was created?	No.
---	-----

Table 16: **VTP Datasheet**. We follow the framework as presented by Gebru et al. [30].

G Credit for visual content

- Figure 1:
 - Row 1: All images are provided under license by Unsplash.
 - Row 2: All images are under the public domain.

- Row 3: First two images are provided under license by Unsplash.
 - Row 5: Available from DALL·E 2 [89].
 - Row 6: First two are provided under license by Unsplash, the third one is provided by Wikimedia Commons, licensed under CC BY-ND 2.0.
 - Row 7: The images are provided by Wikimedia Commons, licensed under CC BY-ND 2.0.
 - Row 8: The images are provided by Wikimedia Commons, licensed under CC BY-ND 2.0.
 - Row 9: This video is from YFCC100M, licensed under CC BY-ND 2.0.
 - Dialogue 1: Available from DALL·E 2 [89].
 - Dialogue 2: The first icon is provided under license by Flaticon, the second image is provided under license by Unsplash, the third one is provided under license by Sketchfab.
 - Dialogue 3: Available from CLIP [85].
 - Dialogue 4: Chicago and Tokyo pictures obtained from Unsplash.
- Model Figures 3, 7, 9 and 8: All images are provided under license by Unsplash.
 - Qualitative Figures 10, 11, 12, and 13: All visuals are sourced from various sources including the COCO dataset, Wikimedia Commons, licensed under CC BY-ND 2.0 or available from DALL·E 2 [89].